Acid mine drainage biogeochemistry at Iron Mountain, California

Gregory K. Druschel[a),b)]
Department of Geology and Geophysics, The University of Wisconsin–Madison, Madison, Wisconsin 53706

Brett J. Baker[a),c)]
Department of Earth and Planetary Sciences, University of California–Berkeley, Berkeley, California 94720

Thomas M. Gihring[d)]
Department of Geology and Geophysics, The University of Wisconsin–Madison, Madison, Wisconsin 53706

Jillian F. Banfield[e)]
Department of Earth and Planetary Sciences, University of California–Berkeley, Berkeley, California 94720

(Received 23 March 2004; accepted 19 May 2004; published online 30 June 2004)

The Richmond Mine at Iron Mountain, Shasta County, California, USA provides an excellent opportunity to study the chemical and biological controls on acid mine drainage (AMD) generation *in situ*, and to identify key factors controlling solution chemistry. Here we integrate four years of field-based geochemical data with 16S rRNA gene clone libraries and rRNA probe-based studies of microbial population structure, cultivation-based metabolic experiments, arsenopyrite surface colonization experiments, and results of intermediate sulfur species kinetics experiments to describe the Richmond Mine AMD system. Extremely acidic effluent (pH between 0.5 and 0.9) resulting from oxidation of approximately 1×10^5 to 2×10^5 moles pyrite/day contains up to 24 g/l Fe, several g/l Zn and hundreds of mg/l Cu. Geochemical conditions change markedly over time, and are reflected in changes in microbial populations. Molecular analyses of 232 small subunit ribosomal RNA (16S rRNA) gene sequences from six sites during a sampling time when lower temperature (<32 °C), higher pH (>0.8) conditions predominated show the dominance of Fe-oxidizing prokaryotes such as *Ferroplasma* and *Leptospirillum* in the primary drainage communities. *Leptospirillum* group III accounts for the majority of *Leptospirillum* sequences, which we attribute to anomalous physical and geochemical regimes at that time. A couple of sites peripheral to the main drainage, ''Red Pool'' and a pyrite ''Slump,'' were even higher in pH (>1) and the community compositions reflected this change in geochemical conditions. Several novel lineages were identified within the archaeal *Thermoplasmatales* order associated with the pyrite slump, and the Red Pool (pH 1.4) contained the only population of *Acidithiobacillus*. Relatively small populations of *Sulfobacillus* spp. and *Acidithiobacillus caldus* may metabolize elemental sulfur as an intermediate species in the oxidation of pyritic sulfide to sulfate. Experiments show that elemental sulfur which forms on pyrite surfaces is resistant to most oxidants; its solublization by unattached cells may indicate involvement of a microbially derived electron shuttle. The detachment of thiosulfate ($S_2O_3^{2-}$) as a leaving group in pyrite oxidation should result in the formation and persistence of tetrathionate in low pH ferric iron-rich AMD solutions. However, tetrathionate is not observed. Although a $S_2O_3^{2-}$-like species may form as a surface-bound intermediate, data suggest that Fe^{3+} oxidizes the majority of sulfur to sulfate on the surface of pyrite. This may explain why microorganisms that can utilize intermediate sulfur species are scarce compared to Fe-oxidizing taxa at the Richmond Mine site. [DOI: 10.1063/1.1769131]

INTRODUCTION

Relevance of the study site

The enhanced oxidation of sulfide minerals principally pyrite (FeS_2), by mining activities is a worldwide problem of significant environmental interest because it leads to the generation of acidic, metal-rich waters. The Richmond Mine, at Iron Mountain in northern California, USA, represents a rare opportunity to study the processes of acid mine drainage underground within an actively oxidizing pyritic body. Where many AMD sites are characterized by precipitation of iron oxyhydroxides, this site is characterized by the dissolved chemical species resulting from microbial pyrite oxidation. Specifically, this field site permits investigation of chemical and microbial factors important in the oxidation reactions that form acidic mine drainage isolated from the part of the system where precipitation of secondary oxyhydroxides occurs. An access tunnel intersects four mine tun-

a)These authors contributed equally to this work.
b)Present address: Department of Geology, University of Vermont, Burlington, VT 05405, Electronic mail: Gregory.Druschel@uvm.edu
c)Electronic mail: bbaker@eps.berkeley.edu
d)Present address: Pacific Northwest National Laboratory, Richland, Washington 99352. Electronic mail: thomas.gihring@pnl.gov
e)Author to whom correspondence should be addressed. Electronic mail: jill@eps.berkeley.edu

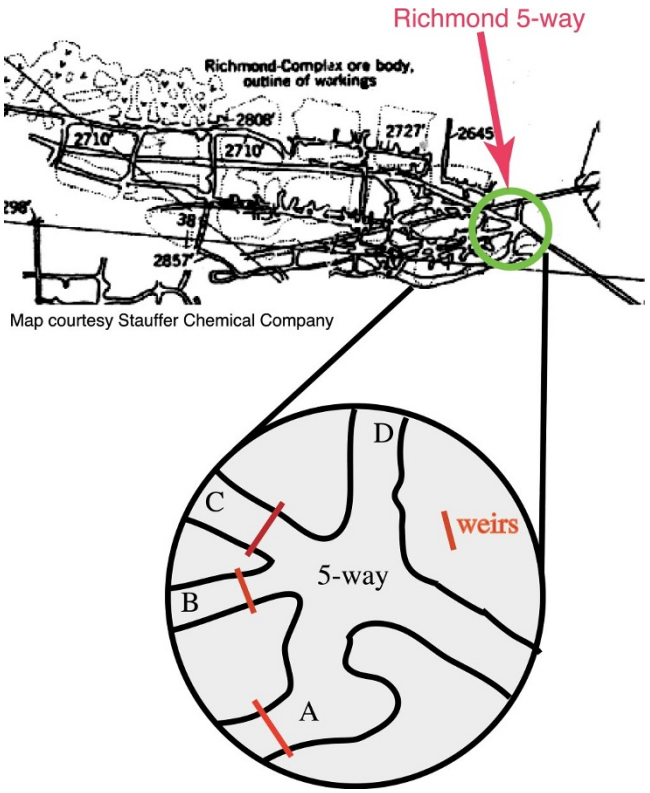

FIG. 1. (Color) Location map of field site at the Richmond Complex 5-way area at the Iron Mountain Superfund Site, northern California, USA. Size of enlarged area is approximately 30 meters in diameter.

nels within the Richmond ore deposit at a junction referred to as the "5-way" (Fig. 1). Essentially all solutions draining from the mine are collected at the 5-way, making it possible to determine and monitor the flux of metals and sulfur from the system. Previous studies of the geology, water chemistry, and microbial communities in the vicinity of the 5-way[1–5] provide the basis for ongoing work at the site.

Site location and history

Iron Mountain is located approximately 9 miles northwest of the city of Redding, California (Fig. 1). Access to the Richmond Mine is provided by a 430 m long horizontal access tunnel that is maintained as part of the United States Government Superfund program remediation effort. The area of the 5-way is located at the edge of the main body of the Richmond deposit, a large, lenticular body that was originally over 800 m long, 60 m wide, and 60 m thick. The body contains approximately 90–95% pyrite (FeS_2), locally enriched with ore minerals. The mine is within a Kuroko-type volcanogenic massive sulfide deposit that contains chalcopyrite ($CuFeS_2$), sphalerite (ZnS), galena (PbS), bornite (Cu_5FeS_4), arsenopyrite (FeAsS), and tetrathedrite–tennantite ($Cu_{12}Sb_4S_{13}$–$Cu_{12}As_4S_{13}$), as well as massive pyrite and late-stage veins of fine-grained pyrite.[6] The ore is hosted in Devonian-age Balaklala Rhyolite composed of quartz, albite, chlorite, and sericite,[7] characterized by very limited acid-buffering capacity. Assays of the pyritic material at the Richmond Mine Complex average 1% copper and 2% zinc.[8] Secondary sulfate minerals associated with the deposit include a variety of Fe^{2+}, Fe^{2+}–Fe^{3+}, and Fe^{3+} sulfates (for details see Alpers *et al.*[2,9]). Several mines were operated intermittently between the 1860s and 1962 for Au, Ag, Cu, Fe, Zn, and pyrite. Of the original reserve estimated at 11.5 million tons, approximately 3.5 million tons were removed.[2] Acidic effluent from the mine was blamed for significant fish kills in the Sacramento river before treatment began.[2] The site has been listed under the National Priorities list for EPA Superfund since 1983[8] and all effluent from the mine is now collected and treated on site by addition of lime (CaO) to remove metals to below the U.S. E.P.A. drinking water standards for Cu (Joe Cobliati, private communication).

Pyrite oxidation and AMD solutions

The oxidation of pyrite proceeds by a transfer of 15 moles of electrons per mole of FeS_2 (converting pyritic sulfide, S^{1-}, to sulfate, $S^{6+}O_4^{2-}$ and Fe^{2+} to Fe^{3+}). Redox reactions occur in increments involving 1 or 2 electrons.[10] Thus, the overall pathway of sulfide oxidation must be composed of many steps. All of the electrons are lost via a series of anodic (oxidizing) half reactions, the sum of which may be represented by:

$$FeS_2 + 8\ H_2O \rightarrow Fe^{3+} + 2\ HSO_4^- + 14\ H^+ + 15e^-, \quad (1)$$

where the product bisulfate is used to represent this reaction occurring below pH 2 [pK_2 of sulfuric acid=1.99 (Ref. 11)] as it likely does at the site. Anodic reactions must be coupled to a cathodic reaction (in the absence of an applied potential). A subset of possible anodic and cathodic reactions describing pyrite oxidation are given in Table I.

TABLE I. Compilation of selected inorganic anodic and cathodic reactions potentially involved with the oxidation of pyrite.

Anodic half reactions	Cathodic half reactions
$FeS_2 + 8\ H_2O \rightarrow Fe^{2+} + 2\ SO_4^{2-} + 16\ H^+ + 14e^-$	$O_2 + 4e^- + 4\ H^+ \rightarrow 2\ H_2O$
$FeS_2 + 3\ H_2O \rightarrow Fe^{2+} + S_2O_3^{2-} + 6\ H^+ + 6e^-$	$Fe^{3+} + 1e^- \rightarrow Fe^{2+}$
$FeS_2 \rightarrow Fe^{2+} + 1/2\ S_4^{2-} + e^-$	$FeOOH + 3\ H^+ + e^- \rightarrow Fe^{2+} + 2\ H_2O$
$FeS_2 \rightarrow Fe^{2+} + 1/4\ S_8 + 2e^-$	$MnO_2 + 4\ H^+ + 2e^- \rightarrow Mn^{2+} + 2\ H_2O$
$FeS_2 + 3\ H_2O \rightarrow Fe^{2+} + 1/2\ S_4O_6^{2-} + 6\ H^+ + 7e^-$	
$FeS_2 + 6\ H_2O \rightarrow Fe^{2+} + 2\ SO_3^{2-} + 12\ H^+ + 10e^-$	
$Fe^{2+} \rightarrow Fe^{3+} + 1e^-$	
$H_2O \rightarrow OH^* + H^+ + e^-$	

Not all coupled redox reactions in the pyrite oxidation pathway generate protons. The reaction producing elemental sulfur, a commonly observed partial product of pyrite dissolution,[12–14] generates no protons:

$$FeS_2 + 2\ Fe^{3+} \rightarrow 3\ Fe^{2+} + 2\ S^0. \quad (2)$$

This reaction represents formation of elemental sulfur directly through the sulfidic sulfur in pyrite. It has been suggested that thiosulfate production at low pH can yield significant elemental sulfur,[15] but recent studies[16] concerning thiosulfate and tetrathionate transformations in acidic waters with excess ferric iron clearly indicate that significant elemental sulfur cannot form from thiosulfate under those conditions. The observation of up to 20% elemental sulfur product in laboratory studies of pyrite oxidation in acidic conditions with excess ferric iron therefore indicates a reaction generating elemental sulfur through another source such as via oxidation of pyritic sulfide.

Thiosulfate has been invoked to be the first product of pyrite oxidation by several researchers.[17–21] Reaction of pyrite over several steps to form thiosulfate (outlined by Luther[17]), which subsequently forms tetrathionate via reaction with Fe^{3+},[16,22] may be represented by the overall reaction:

$$FeS_2 + 7\ Fe^{3+} + 3\ H_2O \rightarrow 8\ Fe^{2+} + 0.5\ S_4O_6^{2-} + 6\ H^+. \quad (3)$$

Reaction of pyrite to form tetrathionate, another intermediate species detected in laboratory pyrite oxidation experiments over a range of conditions,[18,19,21] generates 6 moles of protons per mole of pyrite.

The reaction for the total oxidation of pyrite, assuming that ferric iron is the electron acceptor for all steps, is typically written (for reactions occurring below pH 2):

$$FeS_2 + 14\ Fe^{3+} + 8\ H_2O \rightarrow 15\ Fe^{2+} + 2\ HSO_4^- + 14\ H^+ \quad (4)$$

There is no direct source of ferric iron in AMD systems, so ferric iron must be regenerated from oxidation by oxygen according to the reaction:

$$14\ Fe^{2+} + 3.5\ O_2 + 14\ H^+ \rightarrow 14\ Fe^{3+} + 7\ H_2O. \quad (5)$$

Some reservoirs of Fe^{3+} exist, as pools of dissolved Fe^{3+} and as different ferric sulfate and oxide minerals, which may essentially store this oxidant for varying times before movement/dissolution carries the Fe^{3+} into contact with pyrite surfaces. If reactions (4) and (5) are summed, the overall reaction for pyrite dissolution is given by

$$FeS_2 + 3.5\ O_2 + H_2O \rightarrow Fe^{2+} + 2\ HSO_4^-. \quad (6)$$

If reactions (4) and (5) are exactly balanced to yield reaction (6), the ratio of total iron:protons:sulfate should be 1:2:2. The molar ratio of iron:protons:sulfate will reflect complete oxidation of pyrite if the iron and sulfur are properly accounted (i.e., if no sulfate minerals or iron oxyhydroxide minerals precipitate before sampling the water) and if protons can be properly accounted (i.e., if speciation of protonated forms of carbon, silica, iron, sulfate, etc., can be accounted for). That minerals with mixed-iron valences can precipitate in these waters and that variations in iron oxyhydroxide precipitation can also affect S molar ratios (through precipitation of schwertmannite or sorption of SO_4^{2-} on goethite, for example) emphasize the care required to interpret compositional data.

Although it is clear that proton production is coupled to sulfur oxidation, solution pH is determined by the excess of protons over that required to complex anions (primarily sulfate). If the system is described by reaction (6), sufficient protons would be available to speciate sulfate as HSO_4^-, implying a pH around the pK_1 for HSO_4^-, i.e., ~pH 2. However, not all protons generated by reactions (5) and (6) are required to complex sulfate due to formation of other sulfate complexes (notably Fe^{2+}–sulfate species). Evaporative concentration and precipitation of certain sulfate minerals [e.g., jarosite, $KFe^{3+}{}_3(SO_4)_2(OH)_6$] drives the pH down whereas iron oxidation drives the pH up[23] for solutions at low pH. Modeling results indicate pyrite oxidation can account for lowering pH to approximately 0.0.[24] Under some conditions, extremely low pH values may be attained by evaporative concentration. The lowest pH ever recorded for an environmental sample (−3.6) came from an evaporative pool within the Richmond deposit.[25]

Although oxygen supply ultimately controls pyrite oxidation in the environment, ferric iron is the most efficient oxidant. The lowest unoccupied molecular orbital (LUMO) of Fe^{3+} is lower in energy than the LUMO of O_2 (which typically yields a lower activation energy barrier), which explains why ferric iron is the most effective oxidant.[26] Additionally, O_2 is not as efficient an oxidant due to the spin-restriction of reacting paramagnetic O_2 (2 unpaired electrons) with diamagnetic pyrite (all electrons paired).[18] Because the oxidation of pyrite by Fe^{3+} is so much faster than by O_2, and in view of slow inorganic Fe^{2+} reoxidation rates at low pH, it was proposed that Fe^{2+} reoxidation limits the rate of pyrite oxidation in AMD solutions.[27] Since microorganisms catalyze the oxidation of ferrous iron it was hypothesized that they control pyrite oxidation rates in the environment.[27] Organisms which utilize intermediate sulfur species for metabolic energy are also active in pyrite-oxidizing environments.[28] Microbial populations may change significantly in response to the local environment,[4,29] and between sites of varying acidity.[3] The intermediate reactions governing oxidation of sulfur species may vary with pH, O_2, and Fe^{3+} concentrations as the kinetics of competing reactions depend on the availability of oxidants or the pyrite surface composition. Therefore, understanding differences in the pyrite oxidation pathway as a function of pH may yield better understanding of the interdependence between microbial activity and redox kinetics in acidic environments.

Previous studies of the microbiology of the Richmond deposit

The importance of microbial activity in pyrite dissolution and AMD formation is well documented.[1,19,23,27,30–33] To date, the majority of microbiological studies of AMD systems have been based on physiology and characterization of cultivated organisms. Nordstrom and Southam[32] and Johnson[33] review the concepts that have emerged from these

studies. The key finding is that microorganisms oxidize ferrous to ferric iron, increasing the rate of supply of this important oxidant to the surfaces of dissolving sulfide minerals.

Nordstrom[1] first noted the potential importance of microorganisms at Iron Mountain. Several subsequent studies at the site have applied molecular biological methods to describe the microorganisms present and to correlate microbial community structure with the geochemistry of their environments. Rodgers *et al.*[34] created the first small subunit ribosomal RNA (16S rRNA) gene library from the site (see Edwards[35]). Subsequently, a fluorescent *in-situ* hydridization (FISH)-based study by Schrenk *et al.*[3] determined the relative abundance of archaea, bacteria, and eukaryotes. Schrenk *et al.*[3] also confirmed the findings of Rodgers *et al.*[34] (that *Acidithiobacillus ferrooxidans* is not a significant organism in active AMD generating regions of the ore deposit).

Edwards *et al.*[4] tracked microbial populations over one year and further established the restricted distribution of *At. ferrooxidans*. This study also suggested that another well known Fe-oxidizing acidophile, *Leptospirillum ferrooxidans*, could not account for the majority of microorganisms in most communities sampled. Edwards *et al.*[29] established that archaea are abundant, especially in low-pH, high-ionic strength environments.

A novel, microaerophilic iron-oxidizing archaeon was isolated from the site by Edwards *et al.*[36] This organism comprises up to 85% of the microbial cells in some samples. An isolate, referred to as *Ferroplasma acidarmanus* (strain fer1), is the subject of current detailed physiological (Bond *et al.*[37]) and genomic-based (Allen *et al.*, in prep.) studies. Bond *et al.*[37] analyzed 16S rRNA gene diversity of several specific microenvironments within the Richmond mine. In contrast to Rodgers *et al.*,[34] who targeted planktonic species in AMD solutions and sediments, Bond *et al.*[37] primarily sampled biofilms. The diversity of known archaea, specifically within the order *Thermoplasmatales*, was broadened by this study. Members of the *Thermoplasmatales*, which include clones from the public databases, have been named the ''alphabet plasmas.''[38] Bond *et al.*[37] also identified three distinct phylogenetic groups of *Leptospirillum* (groups I, II, and III). Group II was subsequently named *Leptospirillum ferriphilum*.[39] These findings laid the groundwork for more detailed studies.

METHODS

Geochemical analyses

Field work at the Richmond Mine at Iron Mountain in northern California was conducted over 4 years in the present investigation, as part of a 10-year effort to study the microbial activity associated with metal-sulfide oxidation at this site. Water at the Richmond Mine offers some interesting challenges to the analytical techniques employed in conventional water analyses. Notably, pH standards require special attention to the activity coefficient of H^+ in samples of high ionic strength[25] and oxygen concentration measurements are virtually impossible using standard membrane electrodes or titration methods. On-site analysis of water samples for Eh, conductivity, and temperature were conducted routinely, after established USGS protocols.[40] Standards for pH measurements were prepared from H_2SO_4 stock after the method for measuring extremely low-pH waters developed at the same location by Nordstrom *et al.*[25] A ZoBell's solution was prepared immediately before analysis for a check of the platinum electrode. As noted by Nordstrom,[23] Eh measurements were highly consistent with the Eh calculated from the Fe^{2+}/Fe^{3+} couple (typically within 5%).

Water samples were collected with sterile 60 ml syringes and filtered through 0.2 μm syringe filters into several splits for later analyses. Samples were stored in 15 ml Falcon tubes, filled to occlude any headspace gas, and stored on ice and in a refrigerator until analyses were complete. Ferrous iron was measured on site using a 1,10 phenanthroline method and total iron was measured using a FerroZine method with a Hach portable digital spectrophotometer. In the lab, duplicate splits were measured for Fe^{2+} and Fe^{3+} directly, using the method of To *et al.*[41] and an Ocean Optics UV-Visible spectrophotometer (2000S series). Iron measurements using both methods were consistent within analytical uncertainty, which is primarily due to the high level of dilution necessary for spectrophotometric analyses of these samples. Chromatographic analyses of collected samples for anion determinations were performed on a Dionex Series 500 ion chromatograph equipped with a conductivity detector and UV-Vis detector collected at 230 nm. Sulfate, sulfite, thiosulfate, dithionate, and sulfide were detectable at tens of micromolar levels using an isocratic 5 mM $NaHCO_3$/5 mM Na_2CO_3 eluent at a 1.0 ml/min flow rate through an IonPac AS16 column. Although chloride, phosphate, nitrate, nitrite, and fluoride are also resolvable using chromatographic methods, the extremely high sulfate concentration made quantitative analysis of these ions impossible, given the relatively low concentrations of these species compared to sulfate.

Attempts to measure polythionates were made using an isocratic 30% acetonitrile:H_2O eluent containing 2 mM tetrabulylammonium hydroxide, buffered with 3 mM $NaHCO_3$/3 mM Na_2CO_3 and run through an IonPac NS1 column, modified after several advances in individual polythionate detection by chromatography.[42] Tri-, tetra-, and penta-thionate were all resolvable down to 5 μM concentrations using a 25 μl sample loop. Water samples collected directly from mine effluent, supernatants of samples centrifuged (~4000 rpm) in the field, and water samples preserved on an anion exchange resin after the method of Druschel *et al.*[43] were all analyzed for polythionates and thiosulfate. Elemental sulfur was extracted and analyzed by HPLC using a Shimadzu system UV-Vis at 254 nm, an Alltech C18 column, and an isocratic 95% Methanol:H_2O eluent at 1.0 ml/min after the method detailed in McGuire and Hamers.[44] Trace metals, cations, and silica were analyzed by ICP-MS (VG PlamsaQuad 3), operated in peak jumping mode at the University of Windsor Dept. of Geology. All standards, blanks, and samples were prepared in ultrapure (distilled) 2% HNO_3. Multiple internal standards were used to correct for machine drift that was less than 2% across the mass range.

Mineralogical analyses

Mineral samples from the Iron Mountain Mine site were analyzed by XRD using a Scintag PadV x-ray diffractometer (XRD). Peak matching utilizing the JCPDS Powder diffraction file was used to identify minerals in samples analyzed by XRD. Selected aliquots of cleaned minerals were also analyzed by a LEO 1530 scanning electron microscopy (SEM) and a Cameron SX50 electron microprobe (EMP). Back-scattered electron images and energy-dispersive spectrometer analyses in EMP were utilized to determine enrichments of As, Cu, and Zn in pyritic material.

Geochemical modeling

Geochemical modeling using the Geochemist's Workbench suite of programs[45] was used to calculate speciation in the solutions. Waters from the Richmond Mine have a very high ionic strength. Therefore, proper calculation of the activity coefficients for species of interest requires application of models able to account for interactions beyond simple bimolecular electrostatic interactions, such as the Pitzer equations or HMW models.[46] Speciation calculations of the AMD solutions were carried out using the PHRQPITZ database, which is more accurate in the calculation of activity coefficients for the high-ionic strength solutions at Iron Mountain. However, this database does not include all appropriate ion pairs, especially $FeSO_{4(aq)}$ species. Speciation calculations using PHRQPITZ were carried out using thermodynamic data including available virial coefficients. In an attempt to assess what the errors are with using a database which is missing potentially important species (especially $FeSO_{4(aq)}$), additional and separate calculations were made on these waters using the thermo.dat database provided with the React code of the GWB 3.1.

Particular attention to the total moles of iron, sulfur, and protons in the solution was paid in order to assess iron and sulfur transport and potential sinks relative to the pathways controlling pyrite oxidation and microbial activity in the mine. Analytically, the measured amounts of iron and sulfate accurately reflect the amount of each element in solution. Total H^+ in solution generated from pyrite oxidation is derived from both the free H^+ in solution (from pH and H^+ activity coefficient) and the molar concentrations of protonated species such as bisulfate (which is strongly affected by the abundance of the $FeSO_{4(aq)}$ complex). Bisulfate available to complex H^+ is also affected strongly by iron speciation, as ferrous iron more strongly complexes SO_4^{2-} than does H^+. Results reported for total H^+ are calculated based on the speciation results and are functionally equivalent to the sum of free H^+ and HSO_4^- in solution. There are other species in these solutions, but over 99% of the H^+ is contained in these two species. As such this calculation is slightly different than would be found from an acidity titration because cations which would contain or take up OH^- are not explicitly considered.

Use of GWB 3.1 and the thermo.dat thermodynamic data will result in errors due to extrapolation of equilibrium constants well outside their useful range of ionic strength. There is no current modeling protocol to arrive at a better solution, however. We use H^+ values resulting from these calculations in a strictly qualitative sense, as the error can be greater than 50%, based on comparison of activity coefficients for H^+, HSO_4^-, and $FeSO_{4(aq)}$. Errors in the PHRQPITZ calculations in which total H^+ is comparable to 30-50% of the sulfur species present. Caution should be applied when attemping to use these numbers in anything but a qualitative sense.

Arsenopyrite dissolution and surface colonization studies

The surface colonization and dissolution of pyrite and arsenopyrite by iron- and sulfur-oxidizing micro-organisms from the Richmond Mine have been reported (e.g., Edwards *et al.*[47,48]). Surface-sensitive spectroscopic studies using Raman spectroscopy revealed that elemental sulfur is an important product of the dissolution of pyrite and arsenopyrite.[49,50] In the case of abiotic arsenopyrite dissolution, the majority of the sulfide oxidized is converted to highly insoluble S_8, which accumulates at the mineral surface.[50] Thus, in this study, we conducted experiments designed to explore the interaction between sulfur-oxidizing micro-organisms and the dissolving arsenopyrite surface. These experiments used *At. caldus* because this sulfur-oxidizing organism cannot impact sulfide dissolution via Fe^{2+} oxidation, and thus its primary biogeochemical effect is on the oxidation of intermediate sulfur species such as S_8. An important question to be resolved is whether microbial utilization of sulfur influences sulfide dissolution rates by removal of a diffusion-limiting S_8 coating. Cylindrical Teflon chambers were assembled for three parallel experiments. Chamber 1 was configured with a 0.22 μm pore-size polycarbonate membrane dividing the chamber into two compartments. Each end of the chamber was fitted with a port for removal and addition of material to the compartments. Chambers 2 and 3 were configured in the same manner as Chamber 1, but with no membrane partition in place.

Arsenopyrite preparations and surface-area measurements were carried out as described by McGuire *et al.*[12] Equal portions (by mass) of crushed arsenopyrite were added such that each chamber contained approximately 0.015 m^2 of material. Sections of arsenopyrite polished and cut into $3\times3\times1$ mm coupons were added to Chamber 2 for cell attachment studies. These slabs were placed in perforated 0.5 ml microcentrifuge tubes attached to a Teflon wire extending through the chamber port. The crushed arsenopyrite and the polished coupons were placed into the experiment chambers prior to sterilization by autoclaving. The sterilization techniques likely oxidized the surface of the minerals, but the long-term nature of these experiments with microbial cultures incapable of reduction should not be significantly affected by this.

Each sterilized chamber containing arsenopyrite was filled to half capacity with a total of 210 ml of growth medium. We prepared 9 K medium,[51] modified by omission of $FeSO_4$ and amended with 0.01% (w/v) yeast extract. The medium was adjusted to pH 1.6 and was autoclaved prior to use. Cultures of *At. caldus* TC1 were prepared as previously described[31] to serve as innoculum. The compartment of

Chamber 1 isolated from the arsenopyrite material was inoculated with *At. caldus* cells. Chamber 2 was also inoculated with the same volume of culture (in contact with arsenopyrite material). Chamber 3 was left sterile to serve as an abiotic control. The chambers were incubated in a horizontal position at 37 °C.

Samples for total dissolved iron and cell density measurements were taken from each chamber at prescribed time intervals. One arsenopyrite coupon was retrieved from Chamber 2 during each of the 23, 67, 161, 286, 384, and 477 hour sampling sessions. The coupons were fixed in 3% (w/v) paraformaldehyde for 4 h, rinsed with PBS (phosphate buffering solution), and stored in a 1:1 PBS:ethanol solution at −20 °C.

Total dissolved iron was measured by the FerroZine method. Direct counts of cells in suspension were performed by light microscopy using a Petroff-Hausser counting chamber. Cells attached to arsenopyrite coupons were visualized by staining with DAPI and were viewed using an epifluorescence microscope. Digital images were captured using a CCD camera and the NIH Image software. The area of one image at 1000× was calibrated and 15 random images were counted and averaged for cell density determinations.

Microbial sampling at Richmond Mine

In order to extend prior studies of correlations between microbial populations and geochemical habitats, samples were collected from six sites in the A-, B-, C-drifts and 5-way area (Fig. 1) in January 2001. These were taken from the following locations in the mine; a damp biofilm growing on the surface of a pyrite pile in the A-drift referred to as the ''A-drift Slump'' (01IM1Aslump, pH 1.1), the ''A-drift Red Pool'' (01IM1red pool, pH 1.4), ''A-drift Slime Streamers,'' below the waterfall that separates the ''A-drift Weir'' (01IM1A1, pH 0.9) from the ''5-way'' (01IM1A1, pH 0.89), and biofilms on the ''B-drift Weir'' (01IM1B1, pH 0.75) and ''C-drift Weir'' (01IM1C1, pH 0.85).

Microbiological cultivation

All enrichments contained a basal media consisting of 0.8 g/l $(NH_4)_2SO_4$, 0.4 g/l KH_2PO_4, and 0.16 g/l $MgSO_4$. As carbon sources 0.25 g/l trypcase soy broth (TSB) and 0.2 g/l yeast extract were supplemented to 20 g/l $FeSO_4$ and incubated in 250 ml flasks with vented covers. To enrich for members that can utilize intermediate sulfur compounds 5 mM, thiosulfate, tetrathionate, and S° with 10 mM glucose were added to screw-cap tubes and sealed (with air headspace). The enrichments were incubated at a range of temperatures commonly seen in the mine (24 °C, 37 °C, 45 °C, and 60 °C). All media were pH adjusted to 0.8–1.0. Once growth was observed, $<10^{10}$ dilution series were made to isolate novel organisms.

Construction and analysis of 16S rRNA gene libraries

In January 2001, samples from six sites were collected into sterile containers, placed on ice, and transported back to the laboratory. Samples stored frozen in 25% glycerol were washed in PBS buffer (at pH 1.2 to prevent lysis of obligate acidophiles) to remove extracellular ions. The samples were then resuspended in pH 7.0 PBS, and DNA extractions were carried out as previously described[37] with an additional chloroform wash to remove residual phenol that might inhibit PCR reactions. A suite of domain level primers (27F5′-AGAGTTTGATCCTGGCTCAG-3′; 21Fa5′-TTCC GGTTGATCCYGCCGGAA-3′; A16F235′-TCYGGTTGAT CCTGCC-3′; and 1492R5′-GGWDACCTTGTTACG ACTT-3′) were utilized to amplify 16S rRNA genes from total genomic DNA extract of each of the samples. Specifics of 16S rRNA gene amplification, cloning, sequencing, and analyses of the libraries are provided elsewhere.[52] A few chimeric sequences were found via dual tree comparisons and not included in the final phylogenetic analyses. Sequences were deposited in GenBank under the accession numbers AF543496 through AF543512. Phylogenetic trees were generated using ARB software package and the topologies were confirmed using bayesian inferences as described previously.[52]

FISH (fluorescence *in situ* hybridization) analyses

Samples collected from the same sites, and at the same time as those used for clone library construction, were washed with pH 1.2 PBS buffer and fixed using 4% paraformaldehyde within 12 hours of collection. Hybridization was done following protocols previously reported.[53] Details of all probe synthesis, sequences, and specificity are described elsewhere.[53] Background staining was done to all FISH slides with a DNA stain, DAPI (4′,6-Diamidino-2-Phenylindole Dihydrochloride). Slides were viewed using a Leica LEITZ DMRX epifluorecence microscope. Images were captured with a Hamamatsu digital charge-coupled-device camera using Axiovision software.

RESULTS

Mineralogy

Much of the pyrite ore is fine grained, thus readily liberated from the ore deposit by dissolution. This fine-grained material accumulates as sediment in slumps and on the tunnel floors in layers up to several meters thick in some areas. Analysis by optical and scanning electron microscopy and electron microprobe analyses indicated the sediment is predominantly pyrite with an average particle diameter of ~10–1000 μm. The sediment also contains a few percent quartz. Particle surfaces are roughened by dissolution (Fig. 2). Sulfate minerals (including blue–green melanterite, yellow–brownish jarosite, copiapite, green–blue chalcanthite, pinkish coquimbite, and a compound with cubic crystal form and composition consistent with voltaite) form by evaporative concentration and are locally abundant (inset in Fig. 2).[8] Electron microprobe data indicate that the pyrite particles contain regions that are locally enriched in Zn, Cu, and As. These impurities may account for several percent of the cations in pyrite. No discrete metal sulfide inclusions were observed and no other sulfides were detected in this sediment (although other sulfide phases do occur in the deposit). It is conceivable, however, that the zones of observed Zn, Cu, and

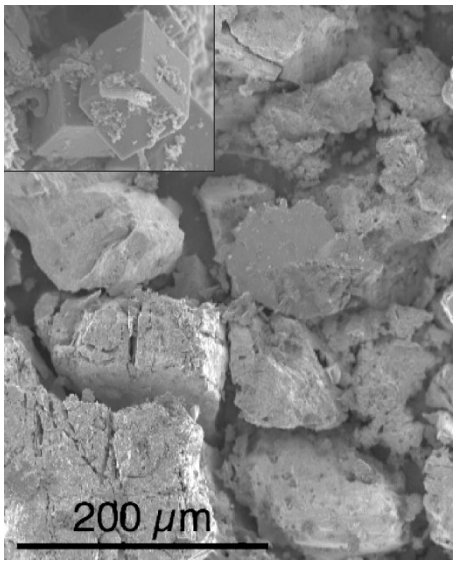

FIG. 2. SEM image of secondary sulfate mineral formation in samples collected within the study site at the Richmond Mine 5-way area. Note sulfate mineral formation on cubic pyrite crystal in the inset.

As enrichment were small inclusions of ZnS, CuFeS, and FeAsS too small to be imaged in the electron microprobe.

Some surfaces of pyrite from the sediments contain deep euhedral pits (Fig. 3). Occasionally very thin, elongated cells occur on the pit base and pit walls. These pitmicrobe associations are very similar to those noted by Edwards *et al.*[35,54] in a SEM study of polished pyrite surfaces of *in-situ* experiments retrieved from the field. In general, the sediment pyrite surfaces are colonized by cells with a limited morphological diversity, suggesting direct interactions involve only a few species.

Arsenopyrite dissolution and surface colonization studies

Acidithiobacillus caldus cells were allowed to directly contact the arsenopyrite in some experiments and were kept separate from the mineral substrate by a 0.2 μm filter in others. As shown by total soluble iron measurements, arsenopyrite dissolution rates were only slightly higher with cells present relative to the abiotic controls [Fig. 4(a)]. Dissolution was most rapid in Chamber 2 where cells were allowed to contact the mineral surfaces. However, the difference in rates between the two biologic and the abiotic reactions is minimal. Given that previous experiments have shown that α-S_8 builds up on the surface during arsenopyrite dissolution,[12,14] the similarity between the abiotic and biotic rates (measured with Fe_T as the reaction progress variable) indicates the absence of dissolution-inhibiting surface products.

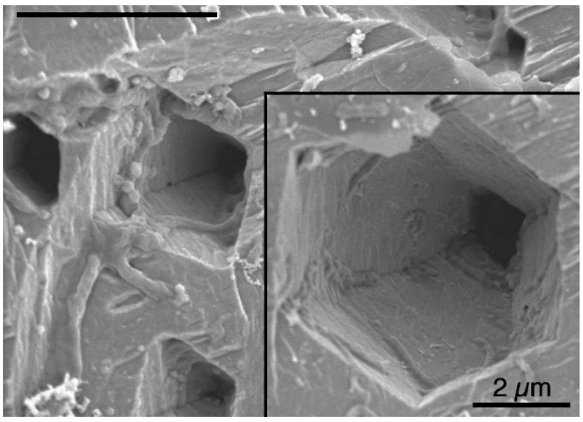

FIG. 3. SEM image of pyrite collected with in study site at the Richmond Mine 5-way area. Note pitted texture of the actively oxidizing pyrite.

At. caldus cells were observed to grow regardless of attachment to the mineral surface [Fig. 4(b)]. This observation suggests that a microbial product may be involved in converting elemental sulfur, which is extremely insoluble under the experimental conditions,[55] into a bioavailable form. This compound may be a shuttle that moves electrons from elemental sulfur to the cell surface. It is unlikely that iron is the electron shuttle as *At. caldus* is unable to oxidize Fe^{2+} and inorganic iron oxidation kinetics are extremely slow under the experimental conditions.

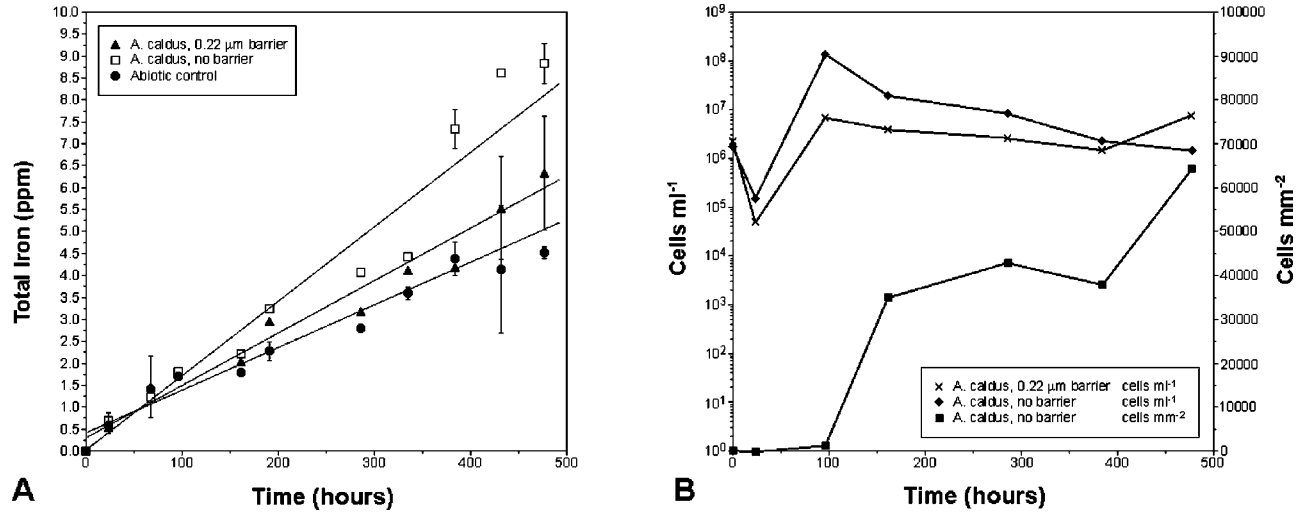

FIG. 4. Results of FeAsS oxidation experiments in which *Acidithiobacillus caldus* was added to reaction vessels and allowed either direct contact with the mineral, or was separated from the mineral with a 0.2 μm filter.

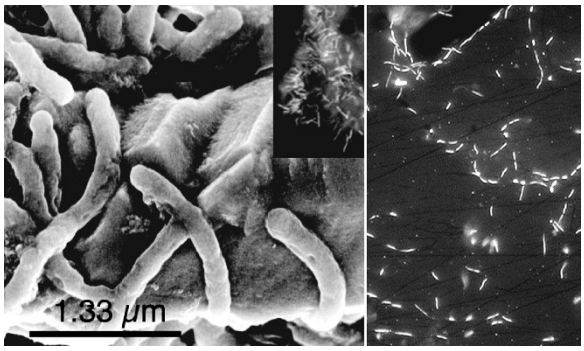

FIG. 5. SEM (left) and DAPI-stained epiflourescence microscopic images of biofilms collected within the study site at the Richmond Mine 5-way area. Note the rod morphology of organisms coating actively oxidizing pyrite grains.

Microbiology

Biofilms, and subaqueous and water surface streamer occur in the 5way area (Fig. 5). Microscopic observations indicate variable numbers of micro-organisms associated with the pyritic sediment. No simple trend between cell numbers and depth of sample site within the sediment was noted.

Tables II and III list the Fe^{2+}, Fe^{3+}, SO_4^{2-}, Cu^{2+}, Zn^{2+}, Al^{3+}, As_T, Ca^{2+}, Cd^{2+}, K^+, Mg^{2+}, Mn_T, Na^+, Pb_T, and SiO_2 concentrations at the sites where microbial samples were collected. Insufficient fluid was available for analysis at the A-drift slump in 2001, and only one sample was collected from the A-drift samples because they are separated by only a few meters of flow path.

Because of PCR bias, clone abundances cannot be used as a proxy for species abundance. Consequently, *in-situ* hybridization studies using probes designed to bind specifically to RNA of organisms detected via clone library analysis were conducted. Due to the high cell density of most samples, the probe-based studies are only semiquantitative. A representative image is shown in Fig. 6, which highlights the *Sulfobacillus* cells in a biofilm. Results confirm earlier deductions[5] that the number of distinct organism types (a type being a phylotype with generally >97% homology in the sequence of the 16S rRNA) is small.

Cultivation-based studies

After several months of incubation on selected intermediate sulfur compounds (thiosulfate, tetrathionate, and S°) no growth was detected. Enrichments containing yeast extract and TSB often resulted in growth. Dilutions of these cultures largely resulted in isolation of *Ferroplasma*. Some *Sulfobacillus* isolates were obtained on yeast extract and $FeSO_4$. Figure 7 shows the phylogenetic placement of three isolates obtained on heterotrophic (yeast extract as a carbon source) media at 37 °C from the mine (SB6 and SB37) that are very closely related to previously characterized organisms (*S. thermosulfidooxidans* VKM and *S. disulfidooxidans*) and clones (see below, BW7). Attempts to grow isolate SB37 on S° were unsuccessful.

Cultivation-independent molecular studies

As shown in Table IV, 232 clones from six libraries were obtained from spatially separate microenvironments sampled in January 19, 2001. No more than six distinct organism lineages were detected in any sample. Previous studies have also shown that AMD communities are characterized by a

TABLE II. Water chemistry of samples collected within the study site at the Richmond Mine 5-way area (at the 5-way, A, B, C weirs, and at the A-slump and red pool in 2001). Concentrations are reported in millimolar units.

Sample name	Date	*T* (°C)	pH	Total H^+	Fe^{2+}	Fe^{3+}	Fe_T	Eh (mV)	Cu	Zn	SO_4^{2-}
99IM25-way	May-99	45	0.71	740	344	31	375	708	6.2	22.4	786
00IM15-way	June-00	36	0.60	761	159	23	182	720	3.2	19.4	743
01IM15-way	January-01	29	0.84	558	64	165	229	794	2.0	16.5	657
02IM15-way	March-02	42	0.83	587	297	20	317	700	4.0	14.3	684
99IM2A1	May-99	38	0.85	566	360	27	387	703	6.4	16.4	824
00IM1A1	June-00	38	0.60	688	107	9	115	705	3.1	11.5	606
01IM1A1	January-01	30	0.89	441	81	177	258	790	2.1	11.3	560
02IM1A1	March-02	42	0.83	579	269	50	319	727	4.1	14.0	665
99IM2B1	May-99	38	0.52	1167	380	41	420	713	5.4	27.9	1161
00IM1B1	June-00	31	0.60	1000	209	61	271	738	3.5	25.3	1020
01IM1B1	January-01	27	0.75	715	55	257	312	810	1.4	25.5	929
02IM1B1	March-02	47	0.78	582	261	13	274	692	2.2	16.8	550
99IM2C1	May-99	48	0.76	805	372	30	403	705	6.0	26.8	1020
00IM1C1	June-00	44	0.60	858	170	25	196	721	3.3	23.8	756
01IM1C1	January-01	32	0.85	503	47	195	243	806	2.0	24.1	635
02IM1C1	March-02	50	0.76	800	281	7	288	676	4.7	14.3	651
02IMM B-back	March-02	45	0.83	544	240	1	241	638	2.3	17.2	586
02IM1 C-back	March-02	50	0.82	583	274	12	286	689	4.5	14.2	656
00IM1 A-slump	June-00	32	1.10	190	26	21	46	764	0.9	1.3	149
01IM1 A red pool	January-01	30	1.38	115	10	25	35	793	0.3	2.7	142
02IMM A-back	March-02	42	0.83	675	363	16	380	690	6.0	18.4	892

TABLE III. Water chemistry of samples collected within the study site at the Richmond Mine 5-way area (at the 5-way, A, B, C weirs, and at the A-slump and red pool in 2001). Concentrations are reported in millimolar units, nd=not determined.

Sample name	Date	Al	As	Ca	Cd	K	Mg	Mn	Na	Pb	SiO_2
99IM25-way	May-99	54	1.6	5.9	0.14	nd	32	0.31	7.8	0.017	nd
00IM15-way	June-00	29	0.9	2.9	0.07	nd	17	0.15	4.5	0.009	nd
01IM15-way	January-01	nd	0.316	nd	0.067	nd	nd	nd	0.596	nd	0.2
02IM15-way	March-02	64	2.0	8.1	0.11	nd	32	0.31	11.8	0.026	nd
99IM2A1	May-99	61	1.2	6.1	0.10	nd	37	0.33	6.6	0.015	nd
00IM1A1	June-00	47	0.4	3.3	0.05	3.3	26	0.24	1.5	0.047	1.3
01IM1A1	January-01	nd	0.3	nd	0.04	nd	nd	nd	0.5	0.036	nd
02IM1A1	March-02	63	1.5	6.8	0.10	nd	31	0.31	11.0	0.018	nd
99IM2B1	May-99	57	1.7	6.2	0.15	nd	30	0.31	9.2	0.019	nd
00IM1B1	June-00	34	0.9	2.9	0.08	nd	17	0.16	5.4	0.011	nd
01IM1B1	January-01	nd	0.4	nd	0.09	nd	nd	nd	0.6	0.018	nd
02IM1B1	March-02	nd	nd	nd	nd	nd	nd	nd	nd	nd	nd
99IM2C1	May-99	51	0.8	3.8	0.13	3.4	29	0.29	2.5	0.046	1.5
00IM1C1	June-00	41	0.6	3.2	0.10	2.7	23	0.23	1.9	0.039	1.3
01IM1C1	January-01	nd	0.4	nd	0.10	nd	nd	nd	0.5	0.039	nd
02IM1C1	March-02	65	1.8	8.1	0.10	nd	33	0.29	15.6	0.02	nd
02IMM B-back	March-02	35	nd	7.3	0.11	nd	17	0.18	12.1	0.023	nd
02IM1 C-back	March-02	67	nd	7.8	0.07	nd	32	0.29	16.0	0.02	nd
00IM1 A-slump	June-00	3	0.2	1.9	0.00	nd	2	nd	0.2	0.015	1.0
01IM1 A red pool	January-01	nd	0.0	nd	0.01	nd	nd	nd	0.2	0.006	nd
02IMM A-back	March-02	80	2.5	10.2	0.13	nd	43	0.38	13.6	nd	nd

limited number of taxonomic groups.[38] Clones belonging to *Nitrospira, Bacillales, Alphaproteobacteria, Deltaproteobacteria, Gammaproteobacteria, Actinobacteria, Acidobacteria*, and the archaeal ''alphabet plasma'' groups were identified and near complete 16S rRNA gene sequences were obtained (Fig. 7). Some of these lineages are closely related to sequences that were previously published from the Richmond mine[37] and a forested wetland site (U.S. Dept. of Energy's Savannah River Site) impacted by acid solutions derived from coal[56] (see coal refuse clones in Fig. 7).

The novel *Deltaproteobacteria* were found solely in A-drift Slump and Red Pool samples. *Leptospirillum* group III was ubiquitous in the communities sampled in this study. *L. ferriphilum* (group II) clones were only found in the A-drift Slump sample. The result distinguishes the microbial communities present at these locations in January 2001 from those detected in previous work.[5]

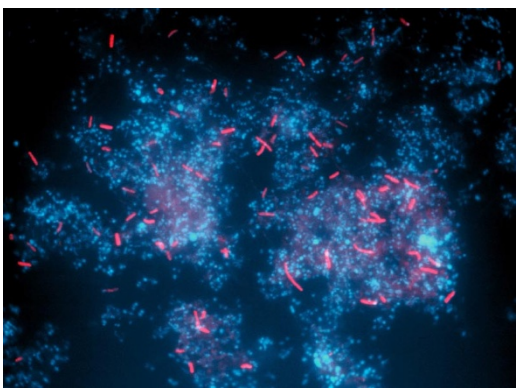

FIG. 6. FISH analyses of *Sulfobacillus* rods in B-drift Weir biofilm on January 2001. Sul228 probe (Ref. 53) is shown in red and DAPI in blue.

Clones significantly divergent from those previously identified (>93% 16S rRNA gene sequence identity) within the order *Thermoplasmatales* were sequenced from A-drift Slump and A-drift Slime Streamer samples. All of these clones fall within the A, B, C, and ''Dplasma'' subgroups (Fig. 7) as defined by Baker and Banfield.[38] These ''alphabet plasma'' are restricted to the lowest pH environments (i.e., they were not found in the pH 1.4 A-drift Red Pool). Other novel lineage related to the division *Actinobacteria* were detected, including clone ASL8 which has 91% 16S rRNA gene sequence similarity with that of a Rheims *et al.*[57] clone TM214.

Sulfobacillus acidophilus-like clones were recovered from all but the A-drift Slump and Slime Streamers. FISH analyses confirmed their presence in several locations, including the A-, B-, C-drift Weir communities (Fig. 6). A lineage not previously associated with the Richmond Mine, closely related to *Sulfobacillus disulfidoxidans* SD-11, was detected in the clone library from the B-drift Weir sample. Furthermore, an isolate belonging to this group was obtained (SB37).

A new group of *Alphaproteobacteria* was identified in the A-drift Red Pool and A-drift Slump libraries. The *Alphaproteobacteria* are directly associated with the protists.[52]

The 16S rRNA gene library from the more oxidized, pH 1.4, A-drift Red Pool is distinct in that it contains a high abundance (21 of 37 total) of *At. ferrooxidans* (Table IV). The Red Pool is also the only location where group I *Leptospirillum*, and *Acidobacteria* were detected. Fluorescent *in-situ* hybridization (FISH) analyses confirmed that *At. ferrooxidans* predominates and that *Acidobacteria* were present in low numbers in the Red Pool (data not shown). Finding *At. ferrooxidans* only in higher pH environments is consis-

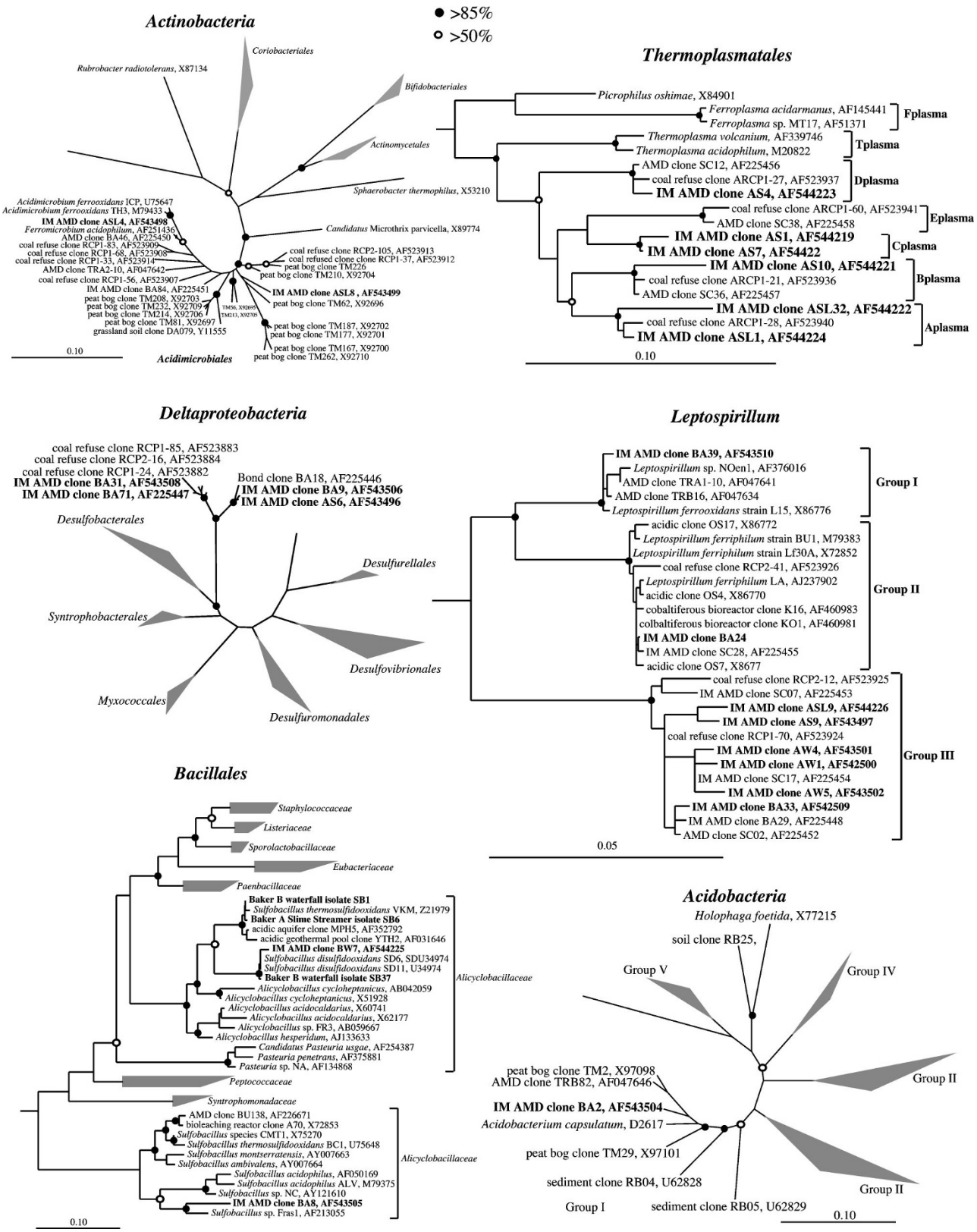

FIG. 7. Phylogeny of 16S rRNA gene sequences from the mine on January 2001 sampling. Tree generated using maximum likelihood (FastDNAM1) in ARB package method. Distance bootstraps values are labeled at their corresponding nodes. Bar represents 0.1 changes per site or 10% difference in nucleotide sequences.

tent with oligonucleotide probe-based studies of Schrenk *et al.*[3] Microscopic investigations of the A-drift Red Pool samples also revealed the presence of protists. This sample and others are the focus of current eukaryotic studies.[58]

Water chemistry

Tabulated results of field and laboratory analyses of water samples collected from the Richmond Mine on 05/11/1999, 06/12/2000, 01/19/2001, and 03/12/2002 are presented

TABLE IV. List of 16S rRNA gene sequences and their taxonomic affiliations (based on BLAST searches of NCBI GenBank database) from the January 19, 2001 sampling. n.i.=not included in phylogenetic analyses.

Mine site	Clones in Fig. 7	Closest match	Similarity	Classification	No. of clones
01IM1-A drift "red pool"	n.i.	*Acidithiobacillus ferrooxidans*	99%	*Gammaproteobacteria*	21
	BA33	Bond clone BA29 (*Leptosprillum* group III)	97%	*Nitrospira*	7
	BA24	*Leptospirillum ferriphilum*		*Nitrospira*	4
	BA39	*Leptospirillum ferrooxidans* strain 49879	99%	*Nitrospira*	3
	BA8	*Sulfobacillus* sp. Fras1, AF213055	94%	*Bacillales*	3
	BA9, BA31, BA71	Iron Mountain Bond clone BA71	99%	*Deltaproteobacteria*	3
	BA2	Uncultured eubacterium WD247, AJ292581	95%	*Acidobacteria*	1
A drift slump	AS10	Uncultured coal refuse clone ARCP1-21	96%	Bplasma, *Thermoplasmales*	6
	AS1, AS7	Uncultured coal refuse clone ARCP1-21	93% and 95%	Cplasma, *Thermoplasmales*	5
	AS4	Uncultured coal refuse clone ARCP1-27	98%	Dplasma, *Thermoplasmales*	4
	AS9	Bond clone BA29 (*Leptosprillum* group III)	98%	*Nitrospira*	7
	AS6	Iron Mountain Bond clone BA18	98%	*Deltaproteobacteria*	3
	n.i.	Iron Mountain Bond clone BA71	99%	*Deltaproteobacteria*	1
	n.i.	*Leptospirillum ferriphilum*	97%	*Nitrospira*	2
	Several (Ref. 38)	*Ferroplasma acidarmanus*	>98%	*Thermoplasmales*	1
A drift slime streamers	Several (Ref. 38)	*Ferroplasma acidarmanus*	>98%	*Thermoplasmales*	20
	ASL9	Bond clone BA29 (*Leptosprillum* group III)	98%	*Nitrospira*	18
	ASL1, ASL32	Uncultured coal refuse clone ARCP1-28	97% and 98%	Aplasma, *Thermoplasmales*	8
	ASL8	Rheims clone TM214	91%	*Actinobacteria*	3
	ASL4	*Ferromicrobium acidophilum*	98%	*Actinobacteria*	1
	Baker *et al.* (Ref. 52)	Endosymbiont of *Acanthamoeba* sp. TUMK23	92%	*Alphaproteobacteria*	2
01IMA1 (A drift weir)	Several (Ref. 38)	*Ferroplasma acidarmanus*	>98%	*Thermoplasmales*	14
	AW1, AW4	Bond clone BA29 (*Leptosprillum* group III)	98% and 99%	*Nitrospira*	13
	Baker *et al.* (Ref. 52)	Endosymbiont of *Acanthamoeba* sp. TUMK23	92%	*Alphaproteobacteria*	2
	n.i.	*Sulfobacillus* sp. Fras1, AF213055	94%	*Bacillales*	1
01IM1B1 (B drift weir)	Several (Ref. 38)	*Ferroplasma acidarmanus*	>98%	*Thermoplasmales*	26
	n.i.	Bond clone BA29 (*Leptosprillum* group III)	98%	*Nitrospira*	21
	n.i.	*Sulfobacillus* sp. Fras1, AF213055	94%	*Bacillales*	2
	BW7	*Sulfobacillus disulfoxidans* SD-11, U34974	99%	*Bacillales*	1
01IM1C1 (C drift weir)	n.i.	Bond clone BA29 (*Leptosprillum* group III)	98%	*Nitrospira*	18
	Several (Ref. 38)	*Ferroplasma acidarmanus*	>98%	*Thermoplasmales*	13
	n.i.	*Sulfobacillus* sp. Fras1, AF213055	94%	*Bacillales*	5

in Tables II and III. No intermediate sulfur species (including aqueous sulfide, thiosulfate, polythionates, or elemental sulfur) were within detection limits in any of the samples.

Table V lists the Fe:S:H^+ ratios calculated using the Geochemist's Workbench for several samples at the mine. Total H^+ was calculated using the GWB 3.1 program React, but the ability of the algorithms to accurately represent the H^+ load is hampered by errors in the calculation of the activity coefficient for H^+ (see discussion in methods section, above). Comparing speciation for calculations using the thermo.phrqpitz database and the thermo database indicates that only a first-order determination of the total H^+ in the solutions can be made.

DISCUSSION

Microbial communities in the Richmond Mine

The study sites located within the mountain are colonized by microbial communities sustained by iron and sulfur oxidation. The microorganisms derive all essential nutrients (phosphate and other ions), materials (CO_2,O_2,N_2), and energy from air, pyrite, and the acid mine drainage solutions. Although the mixture of organisms in individual biofilms varies, most communities are constructed from the same relatively limited set of organism types, many of which have cultivated representatives. Based on physiological measurements for isolates from the Richmond Mine (*F. acidarmanus*,[36] and Baumler *et al.*;[59] *L. ferriphilum* group II, Smriga, unpublished; Lo *et al.* unpublished; *Sulfobacillus* spp. Baker *et al.*, unpublished; *At. caldus*[4]), published measurements for closely related species (*Acidithiobacillus* spp.,[60] *Acidimicrobium* spp.,[61] *Ferromicrobium* spp.,[62] *Leptospirillum ferriphilum*[39,63] and inferences based on phylogenetic placement (*Leptospirillum* group III and the "alphabet plasma"), most of the prokaryotes contribute to AMD generation, either through regeneration of ferric iron oxidant or via metabolism of intermediate sulfur compounds.

We have documented changes in microbial community structure between locations within the mine, and over time. The structure of communities and levels of activity of members is certainly closely tied to geochemical factors, which vary with the seasons. For example, periodically high temperatures typically correspond with periods of high rainfall whereas high ionic strength correlates with low-flow periods. The community structure can also be shaped by non-

TABLE V. Fe:S:H^+ ratios for the samples collected within the study site at the Richmond Mine 5-way area (at the 5-way, A, B, C weirs, and at the A-slump and red pool in 2001).

Sample name	Fe	S	H^+
99IM25-way	1	2.1	2.0
00IM15-way	1	4.1	4.2
01IM15-way	1	2.9	2.4
02IM15-way	1	2.2	1.9
99IM2A1	1	2.1	1.5
00IM1A1	1	5.3	6.0
01IM1A1	1	2.2	1.7
02IM1A1	1	2.1	1.8
99IM1B1	1	2.8	2.8
00IM1B1	1	3.8	3.7
01IM1B1	1	3.0	2.3
02IM1B1	1	2.0	2.1
99IM2C1	1	2.5	2.0
00IM1C1	1	3.9	4.4
01IM1C1	1	2.6	2.1
02IM1C1	1	2.3	2.8
00IM1 Aslump	1	3.2	4.1
01IM1A2	1	4.1	3.3
02IM1A-back	1	2.3	1.8
Average, 1999	1	2.4	2.1
Average, 2000	1	4.0	4.6
Average, 2001	1	2.9	2.1
Average, 2002	1	2.2	2.1
Average, all analyses	1	2.9	2.8

geochemical factors related to biomass concentration, including fungal growth, phase predation, and grazing by protists.[64] These are in turn affected by temperature and solution concentration. In order to evaluate the coupling between the many processes that control AMD generation rates we examine the physical and chemical processes that are the foundation for the biogeochemical system.

The net effect of geochemical and microbial processes

The Richmond Mine AMD effluent is extremely acidic and metal rich because the hydrologic, microbiological, and geologic conditions favor rapid oxidation of large amounts of pyrite. The low pH ($\sim$0.5) of the AMD discharge was modeled by Alpers *et al.*,[2] who noted that approximately 2000 tons of pyrite is dissolved from the Richmond deposit per year ($\sim 1.6\times10^7$ moles or a daily average flux of $\sim 4.4\times10^4$ moles/day). Using the flow data available at the mine flow meter (recorded on days of sampling at the Richmond Mine outflow pipe—collected primarily at the 5-way) and the measured iron concentrations for 5-way samples, the flux of metal coming out of the mine at the 5-way may be determined for that specific sampling period. For the four sampling points in our study, the flux at the 5-way is equivalent to dissolution of between approximately 1×10^5 to 2×10^5 moles FeS_2/day, in good agreement with the average values of Alpers *et al.*[2] considering the significant variability of these data over seasonal scales.

Fe:S:H^+ ratio

As noted above and in Eq. (6), the ratio of iron to sulfate to protons predicted for the complete oxidation of pyrite to sulfuric acid is 1:2:2. Using the chemical data in Tables III and IV (where total H^+ was calculated with GWB as noted in the methods section), we calculated the Fe:S:H ratio at the study sites for each sampling trip. The Fe:S:H^+ values in Table V have an error of approximately ±0.4 for the H^+ value in the ratio for most samples. It is critical to again note that due to the difficulties of properly defining total H^+ only a qualitative discussion of gross differences in this ratio between different sampling times and between different locales sampled at the same time is possible. As an example, comparing ratios of 1:2.1:2.0 with 1:2.5:2.0 would be inappropriate whereas comparing ratios of 1:2.1:2.0 with 1:4.1:4.2 would be appropriate given the error associated with the H^+ calculations.

For most sites at most times the ratio Fe:S:H^+ is close to 1:2:2. Deviation of this value (outside experimental and calculational error) from 1:2:2 may be due to

(1) incomplete oxidation of the pyritic sulfide (e.g., to α-S_8 or another sulfoxyanion less oxidized than SO_4^{2-}),
(2) incomplete reoxidation of Fe^{2+} to Fe^{3+},
(3) net precipitation or dissolution of one of the many iron sulfate minerals found in the Richmond Mine,[9]
(4) dissolution or precipitation of silicates, clays, other sulfate minerals,

(5) precipitation or dissolution of iron oxyhydroxide minerals, or
(6) mixing with another solution affected by (1)–(4).

Incomplete oxidation of pyritic sulfur (e.g., formation of elemental sulfur) can significantly change the H^+ balance in solution [e.g., Eqs. (2) and (3)]. Large amounts of S_8 retained on surfaces may also affect the solution Fe:S:H^+ (most other intermediate sulfur species are quite soluble). Incomplete re-oxidation of $x\,Fe^{2+}$ to Fe^{3+} (as the primary oxidant) increases the amount of H^+ in the system [Eq. (5)], and would raise the H^+ ratio by $1:2:2+x$.

Sulfate mineral precipitation/dissolution may affect Fe, S, and/or H^+ budgets, depending on which sulfate minerals are involved. There are a variety of sulfate minerals that have been observed in the study area (for a thorough review, see Jambor *et al.*[65]) and each may affect overall solution chemistry very differently. For example, jarosite ($KFe_3(SO_4)_2(OH)_6$) precipitation will drive pH down, while rhomboclase precipitation ($(H_3O)Fe(SO_4)_2\cdot 3H_2O$) will drive pH up. Perturbation of the Fe:S ratio is more significant however, as sulfate minerals are either 1:1 ferrous salts or 1.x:1 mixed ferrous–ferric sulfate minerals (no combination approaches the 1:2 ratio of pyrite, as the charge of sulfate is twice that of pyritic sulfide).

Other minerals associated with the Balakla rhyolite and mineralization events are also dissolved, as evidenced by the amounts of soluble Al^{3+}, Ca^{2+}, Mg^{2+}, and other ions in these samples. Rhyolite dissolution does affect the proton budget of the solutions; for example, the reaction of anorthite would consume 8 protons per mole, releasing 1 mole of Ca^{2+}, 2 moles of Al^{3+}, and 2 moles of $SiO_{2(aq)}$. The significant amount of Al^{3+} in these waters may impact the Fe:S:H^+ ratio by consuming some of the H^+ (up to approximately 200–250 mmolar, which can be up to ~30–50% of the total H^+ in some samples).

Ferric oxyhydroxide precipitation/dissolution will affect the Fe_T reservoir and pH. However, most solutions observed at Iron Mountain are at a pH well below that corresponding to ferric oxyhydroxide solubility, even with the very high levels of iron present. Only in the A-drift Red Pool (01IM1A2; pH 1.4, Fe:S:H^+ ratio=1:4.1:3.3) and in higher pH environments outside the ore deposit was evidence for FeOOH accumulation noted (see below). The mine there has an overlying gossan layer, indicating remobilization of iron into oxyhydroxide phases in times before mining. The 5-way area differs from most AMD sites because sampling can occur before solutions have had a chance to neutralize and precipitate significant ferric oxyhydroxide minerals.

The observation that the predicted ratio of Fe:S:H^+ of the AMD solutions generally matches that expected based on the overall stoichiometry suggests that the reservoir of sulfate minerals within the mountain is relatively constant, i.e., oxidation of 2000 tons of pyrite each year is not generating a fast-growing sulfate mineral deposit. Sulfate mineral deposits are known to exist within the mine, but the mine also significantly floods on a seasonal basis, dissolving at least part of that away.[8,9] The Fe:S:H^+ ratio was significantly different in the 06/12/2000 sampling trip (closer to 1:4:4). Jarosite precipitation can sequester Fe and S at about a 1:1 ratio, and generate more H^+ to maintain the 1:1 ratio between S and H^+. Yellow materials identified through XRD analysis as jarosite, copiatite, chalcanthite, and coquimbite were found in several places on the floor of the mine in 2000 (data not shown). The 2000 Fe:S:H^+ ratio likely reflects significant sulfate mineral precipitation and indicates that sulfate accumulation is heterogenous over time.

Oxygen flux

Overall Fe:S:H^+ flux out of the mine is ultimately determined by O_2 supply [Eq. (6)]. The requirement for 3.5 moles O_2 per liter of solution to dissolve pyrite and generate 1 M Fe_T solutions puts the oxygen demand in perspective [see Eq. (6)]. The solubility of O_2 at 3000 m elevation, 40 °C, in a 1 molal ionic strength solution is approximately 140 μM.[66] This means that over the course of fluid flow from recharge to discharge at the 5-way, every liter of water must be completely re-oxygenated about 7500 times.

Though the fact that Iron Mountain ''breathes'' is well established and necessary as part of the development of the AMD solutions at the site,[2,25] we know little about the hydrogeology of the Richmond Mine. Certainly there are a number of deficient hydrogeologic domains. Solutions may move along fracture-controlled flow paths, open channels, percolate through the vadose zone in piles of sediment, or move via saturated subsurface flow. The time it takes for a fluid pulse following a rainfall event to be observed at the 5-way was estimated to range from hours to months (P. Ekoniak, private communication) depending upon the saturation state of the cracks through the solid rock and the pores in the pyritic sediment covering the tunnel floors. However, the transit time for individual pulses may be quite variable and the upper limit is possibly on the scale of years to decades for paths through saturated sediment (D. Dodds, private communication).

Based on historical maps, a fluid path length in the hundreds of meters to several kilometers may be approximated. Using this range, we estimate that the solution must be re-oxidized every 1–100 cm along its flow path. Movement of fluids along this path may be very irregular (fluids may sit in pools or pores for long periods of time prior to flushing or move through the deposit quickly), thus the rate and mechanism of reoxidation may vary considerably.

The mechanisms by which O_2 molecules are dissolved into the solution include (i) diffusion: Calculations using estimates of diffusion indicate O_2 penetration distances in the pyrite sediment in the range of mm to cm (the uncertainties are high); (ii) evaporation–condensation. At times of the year when temperatures are high, steam is associated with flowing AMD. Deeper in the mountain where temperatures exceed 50 °C, this may represent an effective water reoxygenation mechanism. Additionally, the rate of reoxygenation in any fluid is affected by the flow and turbulence of the fluid, therefore any calculation of diffusion rates would be a minimum (slowest) estimate of rate.

The shortest residence time for water in the mine is probably in the range of a day to a month; the upper limit may be years to decades. For a transit time of one day, re-

oxidation of the water along the flow path must occur on the order of once every 10 seconds in order to generate a 0.3 M $FeSO_4$ solution. If residence time is on the order of a month, the reoxidation must occur on the order of once every 5 minutes. Assuming a diffusion gradient of 140 μM/mm (assuming the O_2 profile goes from saturated to anaerobic in 1 mm), and taking the diffusion coefficient of O_2 into water as $2.1\times10^{-9}\,m^2\,s^{-1}$,[67] Fickian diffusion of O_2 into water would occur at approximately 3 $\mu mol\,m^{-2}\,s^{-1}$. To consider the timing of reoxidation another way, if a liter of water has a surface area of $100^2\,cm^2$ (1 liter with geometry 100 cm $\times$100 cm$\times$1 mm depth), reoxidation of 140 μmol O_2 would require about 45 seconds. A liter of water with a surface area of $10^2\,cm^2$ (1 liter with geometry 10$\times$10$\times$10 cm depth) would require over an hour to reoxidize 140 μmol O_2. Oxygen flux into the sediment may then be fast enough to support short residence times only if the gradient is extremely steep, which must then be supported by a process that maintains that steep gradient. Such a process is likely a microbial driven oxidation, though qualitative analysis of this is not possible due to the uncertainties involved with knowing cell numbers, diffusive flux, advective transport effects, and the rates of oxidation.

Heat balance

The temperature of the Richmond solutions at the 5-way typically ranges between 30 °C–50 °C (Table III). Deep within the mine temperatures higher than 56 °C are encountered. It has been suggested previously that the heat is generated as the result of exothermic pyrite oxidation.[8] Using the average $[Fe]_{aq}$ as 0.23 M, ~350 kJ (=83 calories) of heat is liberated per liter of solution due to dissolution of 0.23 moles of pyrite. Assuming the heat capacity for these waters is not significantly different from that of pure water and that all heat accumulates in solution, pyrite oxidation can easily account for the temperature of the AMD fluids.

There are several other processes which may contribute to the overall heat budget in the mine, and especially to temperature changes observed in the system associated with high rainfall and increased flow within the system. Assuming that it takes at least a year for the bulk of the fluid to move from the surface to the 5-way, the high temperatures at the 5-way soon after high rainfall (without a significant pH change) could simply be attributed to recharge-driven movement of fluids from hotter regions of the system.

If there are rapid fluid flow pathways that allow mixing between dilute rain water and more acidic solutions, heats of mixing may also be a source of thermal energy. Calculation of the heat generated by mixing of a two different solutions may be estimated by

$$H_{mix}^{(1,2\rightarrow3)} = H(x^{(3)}) - [X^1 H(x^{(1)}) + X^2 H(x^{(2)})], \qquad (7)$$

where the enthalpy of mixing is derived from enthalpies of solutions 1 and 2 of some mole fraction x mixed at some mole fraction X of the total solution, 3 (after Zeleznik[68]). Based on the mole fractions of H_2SO_4 for some of the extremely low pH solutions reported by Nordstrom *et al.*[25] and higher pH solutions more typically found in other AMD areas, the heat from mixing for several hypothetical scenarios can be calculated. A significant amount of very low pH solution mixing with higher pH solution (50% pH −3 +50% pH 2) would be required to even approach the 20 calories per liter needed to raise the solution to observed temperatures. This level of mixing decreases the resulting solution pH more than that observed for the majority of water flowing out of the mine. An alternative scenario might involve mixing of circumneutral rainwater (transported rapidly from the surface without significant reaction or mixing) with films of very low pH pyrite sediment pore solution. In this scenario, 5% pH −3 solution +95% pH 7 solution results in a solution pH of approximately 0.5, but only contributes 1.7 cal to the solution (i.e., enough to raise 1 liter of water 1.7 °C). Therefore, it is assumed that heat from mixing of different solutions at the Richmond Mine is not a significant contributor to the elevated temperatures.

A temperature pulse may also be induced when rainfall which flushes standing pools of oxidized water into adjacent fine-grained pyrite sediment. These pools may be analogous to the red pool (this study) or to evaporative pools, some of which contain 300 mM Fe^{3+}.[25] Flushing of previously stagnant large pools of Fe^{3+}-rich solutions could contribute large amounts of heat to the system through localized, increased amounts of pyrite oxidation. This process may explain the significant temperature differences observed at different times within the Richmond Mine site.

Significant evaporation that occurs within the mine may be a heat sink. At 40 °C, it requires 10.36 calories to evaporate 1 mole of pure H_2O. However, as the volume of air in the mine is not well constrained and because we have no idea of the rate of evaporation–condensation in these systems, it is impossible to evaluate the role this process plays on the heat budget within the mine.

Pathways for pyrite oxidation and implications for microbial metabolism

The microbial community structure is impacted by the pathways for pyrite oxidation, as these determine the number and type of substrates for growth. Microbes that utilize Fe^{2+} as a substrate depend on inorganic and biological reactions that reduce Fe^{3+} (by reaction with sulfur or organic compounds) to close the cycle. The reactivity of different intermediate sulfur species with Fe^{3+} will impact the rate at which Fe^{2+} is regenerated for microbial use as a substrate.

The mechanism of pyrite oxidation has been intensively studied over a range of conditions utilizing a wide array of techniques and theory.[17–19,21,31,69] Figure 8 illustrates several potential pathways through which pyritic sulfide may oxidize to sulfate. We will examine sulfur oxidation at low pH and consider the potential roles that microorganisms may play. For reference, Table VI (and Fig. 9) presents inferences about metabolisms for each species/group of organisms detected at the Richmond Mine site.

Several studies have observed the formation of polysulfides (see Fig. 8) on the pyrite surface.[70,71] Hu[71] suggested that polysulfide is a precursor to elemental sulfur formation on pyrite surfaces exposed to ferric iron at low pH. Elemental sulfur has been shown to form in many pyrite oxidation

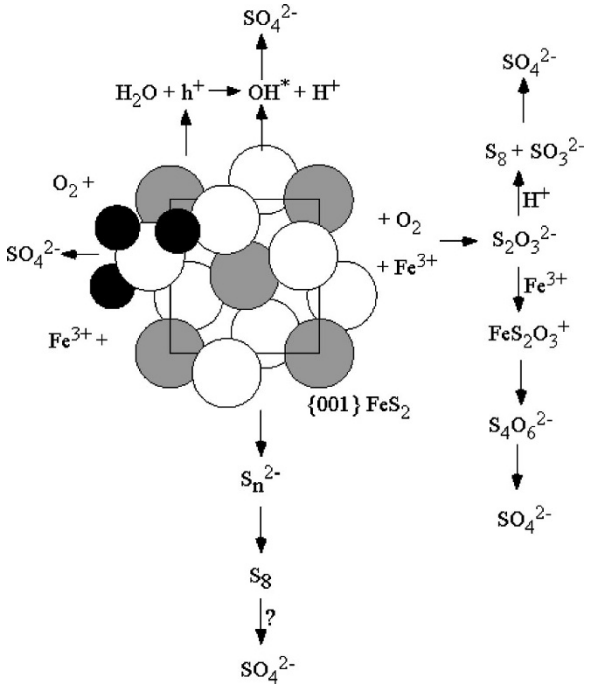

FIG. 8. Diagram representing some of the major potential pathways of pyrite oxidation at low pH.

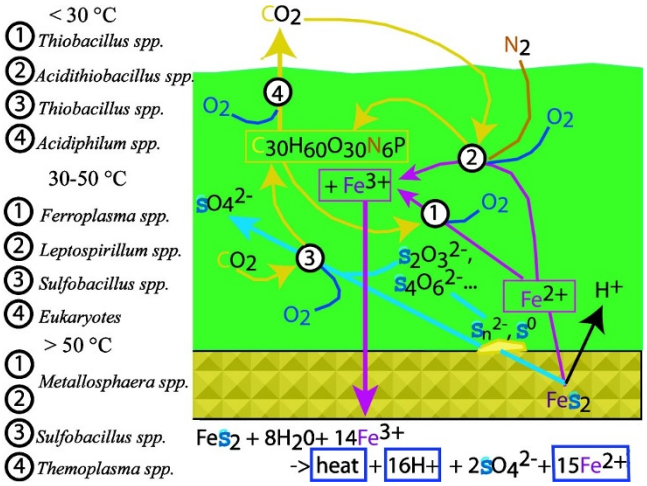

FIG. 9. Schematic diagram of microbial metabolisms prevalent at the Richmond Mine study site.

experiments in variable amounts.[12–14] It has also been shown that the surface-normalized rate of elemental sulfur oxidation under low pH conditions is up to several orders of magnitude slower than the rate of pyrite oxidation.[72] Thus, elemental sulfur should be available for microbial utilization.

There is no evidence for the accumulation of elemental sulfur on pyrite surfaces at the Richmond Mine. *L. ferrooxidans* (groups I and II), which comprise the majority of the community, have not been shown to utilize any S species (Table VI). The *Sulfobacillus* spp. isolates utilize a variety of sulfur compounds as well as organic compounds and other substrates. Although there is evidence for the existence of *Sulfobacillus* spp. in biofilms within AMD solutions and at the solution–air interface, FISH work on sediments did not find significant *Sulfobacillus* populations.[5] *At. caldus* has been isolated from the site (although not commonly detected in clone library-based studies). *At. caldus* can oxidize elemental sulfur without contacting the mineral, suggesting that a shuttle mechanism is important in elemental sulfur oxidation. Electron shuttles refer to small, redox-active organic molecules capable of carrying electrons between reduced and oxidized species as a general mechanism by which microbes may derive energy for cell growth and/or maintenance.[73] Druschel[72] reviews the criteria for potential electron shuttles in this system. Ongoing work is targeted toward identifying and characterizing potential shuttles.

Oxidation of pyrite through the leaving group thiosulfate (A in Fig. 8) is one of the most widely accepted models for the oxidation of pyrite, and is based on experimental evidence[18,21] coupled with a molecular orbital theory description.[17] Subsequent work on the stability of thiosulfate in low-pH solutions similar to those generated during the course of pyrite oxidation indicated thiosulfate decomposition through separate pathways:[15,22,74]

$$4\ S_2O_3^{2-} + 4\ H^+ \rightarrow S_8 + 4\ HSO_3^-, \tag{8}$$

$$2\ S_2O_3^{2-} + 2\ Fe^{3+} \rightarrow FeS_2O_3^+ + FeS_2O_3^+ \rightarrow S_4O_6^{2-} + 2\ Fe^{2+}, \tag{9}$$

$$2\ S_2O_3^{2-} + \tfrac{1}{2}\ O_2 + 2\ H^+ \rightarrow S_4O_6^{2-} + H_2O \quad \text{(pyrite-catalyzed)}. \tag{10}$$

TABLE VI. Microbial metabolisms prevalent in micro-organisms described in the Richmond Mine and their relative abundances defined by FISH and clone library results.

Organism	Metabolic niche in Fig. 9	Number	Autotrophy	$OrgC/O_2$	Fe^{2+}/O_2	S^-/O_2	S_xOyn/Fe^{3+}	$OrgC/Fe^{3+}$
Alphabet plasma		many	n.a.	n.a.	n.a.	n.a.	n.a.	n.a.
Ferroplasma acidarmanus	1, 2	many	yes	yes	YES	no	yes?	n.a.
Acidimicrobium	1, 2	few	yes	yes	yes	n.a.	n.a.	n.a.
Ferromicrobium	1	few	n.a.	yes	yes	n.a.	n.a.	n.a.
Sulfobacillus	1, 2, 4, 7, 8	few	yes	yes	yes	**YES**	**YES**	yes
Leptospirillum ferrooxidans	2, 3	few	yes	no	yes	no	no	no
Leptospirillum ferriphilum	2, 3	many	yes	no	yes	no	no	no
Leptospirillum group III		many	n.a.	n.a.	n.a.	n.a.	n.a.	n.a.
Fungi, protists	5, 6	many	no	**YES**	no	no	no	no

Kinetic modeling of the fate of thiosulfate in solutions analogous to those found at the Richmond Mine indicates that any thiosulfate formed in this environment would oxidize to tetrathionate almost immediately.[38,75] The fate of polythionates in solution was studied in detail by Druschel *et al.*[75,76] Results illustrated that the kinetics of polythionate oxidation coupled to Fe^{3+} or O_2 reduction are slow under acidic conditions. The lack of any observed polythionate species at the Richmond Mine suggests that either pyrite does not oxidize through this pathway, or that microorganisms are present which are able to quickly oxidize the species. Results from the clone libraries (Table IV) and culturing results do not clearly indicate a significant population of microorganisms that directly utilizes intermediate sulfur species. However, it is possible that *Ferroplasma* spp., the ''alphabet plasma,'' and/or *Leptospirillum* group III can couple intermediate sulfur oxidation to reduction of alternate electron acceptors in microaerophilic environments. Based on results for *Ferroplasmsa* strain MT17,[77] *F. acidarmanus* may oxidize intermediate sulfur compounds. Okibe *et al.*[77] suggest that *Ferroplasma* strains MT16 and MT17 are able to utilize tetrathionate as an electron acceptor due to the observation of decreased tetrathionate concentrations after a significant lag phase. However, the growth of one *Ferroplasma* strain in that study ceased at the same time the polythionate concentration decreased and the strains found in the Richmond mine have not demonstrated the ability to utilize intermediate sulfur species as substrate.

The crux of the pyrite oxidation model, where thiosulfate detaches from the surface (Fig. 8), is based on the relative bond strengths of the S–S and Fe–S bonds.[78,79] The comparisons have been made based on bulk values and general observations concerning electron density shifts as a result of oxidation. The strengths of these bonds would certainly be affected by both oxidation processes (bonds affected by loss of *e*- and a decrease in symmetry) and as a result of being at the surface (symmetry decrease). Electron redistribution as a result of these interactions will affect the relative strength of the Fe–S and S–S bonds, which will determine whether $S_2O_3^{2-}$ will detach as a free ion. Experimental observations of the force required to remove $S_2O_3^{2-}$ from a surface,[18] and the lack of significant observed $S_2O_3^{2-}$ or $S_xO_6^{2-}$ at low pH;[13,18,75] suggest that the Fe–S bond is stronger than the S–S bond at low pH. Borda *et al.*[20] have detected thiosulfate-like surface-bound groups on actively oxidizing pyrite, but found no evidence that the species detaches and oxidizes to sulfate in solution. Thus, it seems likely that although the molecular orbital argument of Luther[17] may be correct in large part, the fate of the S_2O_3-like surface group (Fe–S–S–O_3) may not result in appreciable free $S_2O_3^{2-}$ in low-pH conditions. Limited (or no) $S_2O_3^{2-}$ in solution suggests fundamental changes at this step in the oxidation pathway of pyrite as a function of pH. Consequently, microbial utilization of thiosulfate may be affected by whether it is surface bound or released to solution. If thiosulfate remains bound to the pyrite surface (e.g., as Fe–S–S–O_3), then either cells must attach or some other step is required to liberate thiosulfate into solution.

Another possible pathway for pyrite oxidation involves the formation of intermediate oxygen radical species (Fig. 8).[18,79–81] Hydroxyl radicals (OH*) form at the pyrite surface due to dissociation of water (present either as a free species in solution or as part of the hydration sphere of iron) following reaction with a hole (vacancy of an *e*- in a filled energy level; the hole is filled by the electron lost from water).[82] The hole may be created by an oxidation reaction (in solution or in air), a defect, or by a dopant in the mineral. Natural pyrite may include significant impurities, and examples of both *n*- and *p*-type pyrite (*p*-type pyrite has extra holes) are abundant in natural deposits.[79]

Oxidation of pyrite by OH* generates sulfoxy species in which the oxygen is derived from water (consistent with above mentioned isotopic results):

$$FeS_2 + Fe^{3+} \rightarrow FeS_2 + h^+ + Fe^{2+}, \quad (11)$$

$$H_2O + h^+ \rightarrow OH^* + H^+, \quad (12)$$

$$FeS_2 + OH^* \rightarrow FeS_2O^- + H^+ \quad (13)$$

where h^+ is a hole site in the pyrite. In this pathway, oxidation of intermediate sulfur species is rate-limited by the formation of OH*. The formation of OH* is due to intrinsic defects and/or *p*-type dopants is a sulfur oxidation pathway that is independent of oxygen supply.

Most intermediate S species will react with hydroxyl radicals very quickly, with the notable exception of elemental sulfur.[72] The abiotic rate of oxidation of many intermediate sulfur species with OH* is on the scale of microseconds or faster.[76] Thus, the hydroxyl radical pathway in environmental systems may out-compete micro-organisms for the potential energy available from intermediate sulfur species, possibly explaining the apparent scarcity of these organisms within the Richmond Mine system. Generation of additional hydroxyl radicals may be associated with wetting of oxidized surfaces.[72,80] This source of OH* may also affect the distribution of intermediate sulfur species in the mine during times of flooding after dry periods.

As seen in Table I, the source of oxygen in sulfate formed from pyrite-derived sulfide is H_2O for all cathodic reactions except where O_2 is the primary oxidant. Isotopic analyses indicate that the source of most of the oxygen in sulfate derived from pyrite oxidation under laboratory and natural conditions is H_2O and not O_2.[83] However, at low pH sulfite—water isotopic exchange is thought to be very fast and any record of direct O_2 oxidation on previous intermediate sulfur species formed in the course of pyrite oxidation could be erased[84] and is thus not a good indicator of reaction pathways at Iron Mountain.

Toxic metals

Arsenic, Cu, or Zn in the water-transported pyrite accumulations (sediment) in the tunnels may exist as separate mineral grains, small inclusions of discrete minerals within pyrite grains, or as local enrichments. Additionally, these elements are probably heterogeneously distributed in the ore body and may be more abundant in recently exposed ore than in the more weathered sediments.

TABLE VII. Correlation table of selected ions in the 5-way, A, B, and C drifts over the sampling times in Tables II and III. A value of 1.00 is the maximum correlation, and the sign indicates positive or inverse correlation.

	T (C)	pH	Total H^+	Fe^{2+}	Fe^{3+}	FeT	Eh	Cu	Zn	SO_4^{2-}	Al	As	Ca	Cd	Mg	Mn	Na
pH	−0.02																
Total H^+	0.11	**−0.86**															
Fe^{2+}	**0.71**	−0.16	0.41														
Fe^{3+}	**−0.78**	0.41	−0.35	**−0.71**													
FeT	0.28	0.16	0.25	**0.75**	−0.07												
Eh	**−0.85**	0.34	−0.35	**−0.78**	**0.97**	−0.20											
Cu	0.57	−0.18	0.39	**0.90**	−0.64	0.68	−0.68										
Zn	−0.14	−0.47	0.65	0.17	0.17	0.40	0.17	0.18									
SO_4^{2-}	−0.11	−0.54	**0.80**	0.44	−0.04	0.59	−0.07	0.47	**0.80**								
Al	0.62	0.67	−0.37	0.63	−0.20	0.56	−0.61	0.54	−0.40	−0.19							
As	**0.71**	−0.10	0.32	**0.79**	−0.63	0.54	**−0.72**	0.68	−0.06	0.20	**0.70**						
Ca	0.62	0.62	−0.30	0.57	−0.18	0.51	−0.60	0.41	−0.40	−0.24	**0.91**	**0.92**					
Cd	0.53	−0.21	0.51	**0.76**	−0.30	**0.80**	−0.39	**0.70**	0.64	0.64	0.42	0.59	0.39				
Mg	0.59	**0.70**	−0.45	0.69	−0.29	0.61	−0.65	**0.71**	−0.34	−0.17	**0.94**	0.56	**0.79**	0.45			
Mn	0.59	0.60	−0.30	**0.76**	−0.13	**0.70**	−0.52	**0.72**	−0.17	−0.02	**0.94**	0.59	**0.78**	0.61	**0.97**		
Na	0.68	−0.03	0.25	0.68	−0.59	0.42	**−0.70**	0.57	−0.21	0.06	**0.70**	**0.96**	**0.91**	0.43	0.51	0.50	
Pb	0.26	0.00	−0.13	−0.08	−0.07	−0.17	−0.07	−0.02	−0.01	−0.16	0.04	−0.30	−0.27	−0.02	0.09	0.13	−0.31
	T (C)	pH	total H^+	Fe^{2+}	Fe^{3+}	FeT	Eh	Cu	Zn	SO_4^{2-}	Al	As	Ca	Cd	Mg	Mn	Na

Galvanic interactions between sulfide minerals lead to rapid loss of arsenopyrite, chalcopyrite and sphalerite.[85] This galvanic coupling would protect the pyrite cathode while selective anodic dissolution of the other sulfides proceeds. Localized As, Cu, and Zn impurities revealed by EMP analysis will change the pyrite reactivity by affecting its local electronic structure. Selective oxidation of inclusions or enrichment areas may lead to localized pitting, such as observed in Fig. 3, and influence patterns of microbial attachment. The concentrations of toxic metals such as As, Cu, Cd, Hg, and Ag can also influence microbial community structure because different species and strains may have different metal tolerances.

Spatial and temporal variability

Geochemical data from the sampling sites at each weir (A-, B-, and C-drifts) and the 5-way area on four sampling dates are shown in Table II and Table III and the correlation matrix is represented in Table VII. This table lists the Pearson correlation coefficients for each variable vs every other statistically significant variable. Strong correlation of temperature with Fe^{2+}, Fe^{3+}, and Eh illustrates that the heat of pyrite oxidation controls temperature. Strong correlation of H^+ with SO_4^{2-} illustrates the dependence of proton generation on the oxidation of sulfur species in the pyrite-oxidation pathway. Interestingly, Cu correlates with Fe^{2+}, while Zn does not, suggesting different factors control their concentrations. This correlation may indicate release by galvanic reaction, or it could be caused by melanterite dissolution, as the melanterite in this mine is known to contain significant Cu and Zn.[9]

Over time, Eh varies in the drifts in the same manner (Table II). This suggests that perturbations due to seasonal changes affect the entire system consistently, and implies that similar processes are occurring in all drifts and associated stopes.

Anomalously high Eh was observed in 2001. The high rainfall one week prior to the sampling trip may have caused flushing of sulfuric acid-rich films formed on pyrite surfaces and of pools created during dry months, dissolution of sulfate minerals, and introduction of O_2. In time, Fe^{3+} consumption due to pyrite oxidation returned the Eh value to that determined by the balance between O_2 diffusion, surface oxidation reactions, and microbial activity.

The ~0.14 moles/L excess Fe^{3+} observed in solution in January 2001 compared to prior sampling times requires supply of an additional 3.5×10^{-2} moles O_2/L. Even if the entire volume of solution was new rainwater (with 2.5×10^{-4} moles O_2) there is a more than two orders-of-magnitude deficit in O_2 supply. In fact, in order to provide the 3.5×10^{-2} moles O_2/L it is necessary to reoxygenate the solution over 200 times, given the solubility of O_2 in AMD of $<1.40\times10^{-4}$ M. Thus, rainfall alone cannot explain the high Fe^{3+} compared to other sampling times. Other factors that could raise the Eh of the system include alteration of the ferrous/ferric iron ratio due to changes in the rate of advection through the system or in the activity level of Fe-oxidizing prokaryotes.

Geochemical factors controlling microbial community structure

Iron-oxidizing microorganisms are abundant in all communities studied (Bond *et al.*[5] and this study). Aerobic iron-oxidizing microorganisms form conspicuous biofilms (often dominated by *Leptospirillum* spp.) at the sediment- or solution–air interface. Activity within these biofilms generates solutions in which the aqueous ferric iron concentrations are typically several of orders magnitude greater than oxygen concentrations. These solutions percolate into sediments where they induce anaerobic oxidation of pyrite and associated intermediate sulfur compounds. This supply of Fe^{3+} is important for organisms that couple oxidation of S compounds (or organic carbon) to reduction of Fe^{3+} (Fig. 9). The

decoupling of oxygen diffusion from oxidation reactions suggests that oxygen-saturated pyrite sediments are probably populated by microbial communities that are distinct from those growing in aerobic or microaerophilic regions.

Some differences in microbial population composition are observed among the different sampling locations for the January 19, 2001 trip (Table IV). Microbial communities within the more oxidized A-drift Red Pool and at the A-drift Slump are associated with higher pH solutions with generally lower metal and sulfate concentrations (up to 5–10 times lower, see Tables II and III). The geochemical and microbiological characteristics of the Red Pool are most distinctive. The A-drift Red Pool contains the only populations of *At. ferrooxidans, L. ferrooxidans*, and *Acidobacteria*, consistent with the known pH and temperature optima for these bacteria.[39,60,86] The A-drift Slump area contains significant populations of ''alphabet plasma'' (Table IV). These are also present in the A-drift Slime Streamers and the Slump (Table V). As the ''alphabet plasma'' clones are significantly divergent (>7%) from characterized *Thermoplasma* spp. isolates (Fig. 7), which are thermophilic facultative anaerobes,[87] it is not possible to deduce their metabolic roles based on phylogenetic position. Factors that may contribute to proliferation of ''alphabet plasma'' in A-drift Slump slimes are the lower temperatures, higher pH, and high abundance of biofilm polymers. Phylogenetically related *Thermoplasma* have been reported from a wetland impacted by coal refuse with a pH and temperature similar to that of the A-drift Slump.[56]

The clone libraries and FISH results for all sites in the B- and C-drifts are similar, as expected based on general similarities in geochemistry and temperature. Populations are dominated by *Ferroplasma acidarmanus* and *Leptospirillum* (group III) microorganisms. The predominance of *Leptospirillum* group III in January 2001 distinguishes these communities from those previously documented at these sites[5] and Tyson *et al.*[88]). The most likely geochemical control is the unusually high Fe^{3+}:Fe^{2+} in solutions in January 2001, which may imply that the redox potential for electron transport chain enzymes involved in iron oxidation differs between the *Leptospirillum* groups.

It has been noted previously that microbial populations at the site vary substantially in response to seasonal rainfall, which correlates with changes in ionic strength and temperature. Generally, archaeal populations predominate during the drier months when pH and ionic strength are higher, and bacterial and eukaryotic populations are more significant in wetter months.[29,89] The relatively low abundance of archaeal populations in January 2001 is consistent with this conclusion.

CONCLUSIONS

Rainfall, primarily occurring early in the year, introduces a relatively small amount of oxygen that is rapidly consumed by reaction with pyrite within the mine workings and by microorganisms that couple its reduction to oxidation of ferrous iron. The evolving AMD solution must be reoxidized thousands of times along its flow path in order for it to acquire the metal and sulfur load observed as it exits the system. Oxygen diffusion into solution is promoted by microbial respiration. A key role for iron-oxidizing bacteria and archaea in AMD generation is acceleration of the otherwise slow Fe-oxidation reaction (which is particularly slow at low pH), which promotes pyrite dissolution and leads to rapid accumulation of Fe^{2+}, SO_4^{2-}, and H^+ along the flow path. Exothermic pyrite oxidation is the predominant source of heat. However, flushing of very oxidized solutions (formed over the dry summer and fall months) into pyrite sediments may contribute to the heat spike following high rainfall. The ratio of Fe:S:H^+ indicates no consistent accumulation of sulfate minerals, elemental sulfur, or other sulfoxy compounds over extended periods of time. However, seasonal variations may be attributed to sulfate mineral accumulation and dissolution, as noted previously.[9] These results indicate that sulfate minerals in the mine precipitate and dissolve over seasonal time frames, but averaged over time, the effluent generally reflects complete pyrite oxidation.

Microbial communities contain a relatively small number of distinct taxa, as discussed previously.[37,38] Cultivation-independent surveys of microbial communities revealed a few newly recognized lines of descent. Much of the novelty lies within the *Thermoplasmatales* order and *Actinobacteria*, detected primarily within the A-drift subaerial habitats. Only in higher pH, lower metal and sulfate concentration environments were groups such as *Acidithiobacillus ferrooxidans, Acidobacteria* sp., and *Leptospirillum ferrooxidans* found. The apparent predominance of Fe-oxidizing organisms suggests that abiotic pathways of sulfur oxidation are rapid due to the high flux of ferric iron and possibly due to formation of oxygen radicals. However, further metabolic characterization of as yet uncultivated ''alphabet plasma'' and *Leptospirillum* group III species is required in order to test for their ability to oxidize intermediate sulfur species.

At the Richmond Mine, the dominance of iron-oxidizing microorganisms (*Ferroplasma acidarmanus* and *Leptospirillum* spp.) ensures a continual supply of ferric iron, making it likely that all steps along the oxidation pathway of pyrite to SO_4^{2-} involve the oxidation of intermediate sulfur species by ferric iron. The kinetics of thiosulfate and tetrathionate oxidation at these conditions,[22,74–76] suggest that the pathway of pyrite oxidation does not significantly progress through the detachment of thiosulfate in low-pH environments. Bioavailablity of elemental sulfur as an intermediate sulfur species is possible even if the mechanisms of pyrite oxidation include generation of oxygen radicals because elemental sulfur is not readily dissolved via radical pathways tested to date. Some subset of intermediate products (such as elemental sulfur) are resistant to reaction with Fe^{3+} and is open to utilization by *Sulfobacillus* spp. and *Acidithiobacillus caldus*, either through direct contact or through an enzymatic shuttling process that allows the organisms to keep some distance away from the pyrite surfaces. This speculation requires further analysis.

ACKNOWLEDGMENTS

The authors wish to thank Gene W. Tyson, Dr. Philip Hugenholtz, Ian Lo, Dr. Katrina Edwards, Dr. D. Kirk Nordstrom, Dr. Mark Williamson, Dr. George Luther III, Dr.

Martin Schoonen, Dr. Mike Borda, and Don Dodds for helpful discussions in the course of this work. We would also like to thank Ted Arman(us) (Iron Mountian Mines Ltd), Joe Cobliatti, Don Dodds, and Dr. Rick Sugareck (EPA) for allowing access to the study site. This research was supported by Grants Nos. CHE 9521731, CHE 9807598, and MCB 9978205 from the National Science Foundation and LDRD support from Lawrence Berkeley National Laboratory.

[1] D. K. Nordstrom, Ph.D. thesis, Stanford University, 1977.
[2] C. N. Alpers, D. K. Nordstrom, and J. M. Burchard, Water Resources Investigations—U.S. Geological Survey Report Report No. WRI 91-4160, 1992.
[3] M. O. Schrenk, K. J. Edwards, R. M. Goodman, R. J. Hamers, and J. F. Banfield, Science **279**, 1519 (1998).
[4] K. J. Edwards, B. M. Goebel, T. M. Rodgers *et al.*, Geomicrobiology J. **16**, 155 (1999).
[5] P. L. Bond, G. K. Druschel, and J. F. Banfield, Appl. Environ. Microbiol. **66**, 4962 (2000).
[6] A. R. Kinkel, W. E. Hall, and J. P. Albers, U.S. Geological Survey Professional Paper Report No. 285, 1956.
[7] B. C. South and B. E. Taylor, Econ. Geol. **80**, 2177 (1985).
[8] D. K. Nordstrom and C. N. Alpers, Proc. Natl. Acad. Sci. U.S.A. **96**, 3455 (1999).
[9] C. N. Alpers, D. K. Nordstrom, and J. M. Thompson, in *Environmental Geochemistry of Sulfide Oxidation*, edited by C. N. Alpers and D. W. Blowes (American Chemical Society, Washington, DC, 1994), Vol. 550, p. 324.
[10] R. G. Pearson, *Symmetry Rules for Chemical Reactions: Orbital Topology and Elementary Processes*, 1st ed. (Wiley, New York, 1976).
[11] D. R. Lide (CRC Press, Boca Raton, 2004).
[12] M. M. McGuire, K. N. Jallad, D. Ben-Amotz, and R. J. Hamers, Appl. Surf. Sci. **178**, 105 (2001).
[13] A. Schippers, T. Rohwerder, and W. Sand, Appl. Microbiol. Biotechnol. **52**, 104 (1999).
[14] K. Sasaki, M. Tsunekawa, T. Ohtsuka, and H. Konno, Geochim. Cosmochim. Acta **59**, 3155 (1995).
[15] F. Johnston and L. McAmish, J. Colloid Interface Sci. **42**, 112 (1973).
[16] G. K. Druschel, R. J. Hamers, and J. F. Banfield, Geochim. Cosmochim. Acta **67**, 4457 (2003).
[17] G. W. Luther, Geochim. Cosmochim. Acta **51**, 3193 (1987).
[18] C. O. Moses, D. K. Nordstrom, J. S. Herman, and A. L. Mills, Geochim. Cosmochim. Acta **51**, 1561 (1987).
[19] A. Schippers and W. Sand, Appl. Environ. Microbiol. **65**, 319 (1999).
[20] M. J. Borda, D. R. Strongin, and M. A. A. Schoonen (unpublished).
[21] M. B. Goldhaber, Am. J. Sci. **283**, 193 (1983).
[22] M. A. Williamson and J. D. Rimstidt, Geochim. Cosmochim. Acta **57**, 3555 (1993).
[23] D. K. Nordstrom, Int. Geol. Rev. **42**, 499 (2000).
[24] C. N. Alpers and D. K. Nordstrom, Rev. Econ. Geol. **6**, 289 (1999).
[25] D. K. Nordstrom, C. N. Alpers, C. J. Ptacek, and D. W. Blowes, Environ. Sci. Technol. **34**, 254 (2000).
[26] G. W. Luther, in *Aquatic Chemical Kinetics*, edited by W. Stumm (Wiley, New York, 1990), pp. 173; G. W. Luther and J. I. Popp, Aquatic Geochem. **8**, 15 (2002).
[27] P. C. Singer and W. Stumm, Science **167**, 1121 (1970).
[28] P. R. Norris, R. M. Marsh, and E. B. Lindstrom, Biotechnol. Bioeng. **8**, 318 (1986); T. A. M. Johnson and D. B. Bridge, Appl. Environ. Microbiol. **64**, 2181 (1998); J. Kelly and D. P. Mason, Arch. Microbiol. **149**, 317 (1988).
[29] K. J. Edwards, T. M. Gihring, and J. F. Banfield, Appl. Environ. Microbiol. **65**, 3627 (1999).
[30] A. Schippers, P. Jozsa, and W. Sand, Appl. Environ. Microbiol. **62**, 3424 (1996); L. Larsson, G. Olsson, O. Holst, and H. Karlsson, *ibid.* **56**, 697 (1990); K. J. Edwards, M. O. Schrenk, R. Hamers *et al.*, Am. Mineral. **83**, 1444 (1998); W. Sand, T. Gehrke, P. G. Jozsa *et al.*, Hydrometallurgy **59**, 159 (2001); T. A. Fowler, P. R. Holmes, and F. K. Crundwell, *ibid.* **59**, 257 (2001); A. Schippers, P. G. Jozsa, W. Sand *et al.*, Geomicrobiol. J. **17**, 151 (2000); W. Sand and H. von Rege, in *Biofilms* (1999), Vol. 310, p. 361; B. Elberling, A. Schippers, and W. Sand, J. Contam. Hydrol. **41**, 225 (2000); T. A. Fowler, P. R. Holmes, and F. K. Crundwell, Appl. Environ. Microbiol. **65**, 2987 (1999); P. R. Holmes, T. A. Fowler, and F. K. Crundwell, J. Electrochem. Soc. **146**, 2906 (1999); M. Boon and J. J. Heijnen, Hydrometallurgy **48**, 27 (1998); H. Tributsch and J. A. Rojas-Chapana, Electrochim. Acta **45**, 4705 (2000); F. Battaglia-Brunet, P. d'Hugues, T. Cabral *et al.*, Minerals Eng. **11**, 195 (1998).
[31] M. M. McGuire, K. J. Edwards, J. F. Banfield, and R. J. Hamers, Geochim. Cosmochim. Acta **65**, 1243 (2001).
[32] D. K. Nordstrom and G. Southam, in *Geomicrobiology: Interactions between Microbes and Minerals*, edited by K. H. Nealson (Mineralogical Society of America, 1997), Vol. 35, p. 361.
[33] D. B. Johnson, FEMS Microb. Ecol. **27**, 307 (1998).
[34] T. M. Rodgers, Masters thesis, University of Wisconsin, 1996.
[35] K. J. Edwards, Ph.D. thesis, University of Wisconsin, 1999.
[36] K. J. Edwards, P. L. Bond, T. M. Gihring *et al.*, Science **287**, 1796 (2000).
[37] P. L. Bond, S. P. Smriga, and J. F. Banfield, Appl. Environ. Microbiol. **66**, 3842 (2000).
[38] B. J. Baker and J. F. Banfield, FEMS Microbiol. Ecol. **44**, 139 (2003).
[39] N. J. Coram and D. E. Rawlings, Appl. Environ. Microbiol. **68**, 838 (2002).
[40] F. D. Wilde and D. B. Radke, *U.S. Geological Survey TWRI Book 9* (U.S.G.S., 2001), Vol. 9.
[41] T. B. To, D. K. Nordstrom, K. M. Cunningham, J. W. Ball, and R. B. McCleskey, Environ. Sci. Technol. **33**, 807 (1999).
[42] R. Steudel and G. Holdt, J. Chromatogr. **361**, 379 (1986); R. Strauss and R. Steudel, Fresenius' Z. Anal. Chem. **326**, 543 (1987); J. W. O'Reilly, G. W. Dicinoski, M. J. Shaw *et al.*, Anal. Chim. Acta **432**, 165 (2001); S. B. Rabin and D. M. Stanbury, Anal. Chem. **57**, 1130 (1985); H. Zou, Z. Jia, Y. Zhang *et al.*, Anal. Chim. Acta **284**, 59 (1993).
[43] G. K. Druschel, M. A. A. Schoonen, D. K. Nordstrom, J. W. Ball, Y. Xu, and C. A. Cohn, Geochem. Trans. **4**, 12 (2003).
[44] M. M. McGuire and R. J. Hamers, Environ. Sci. Technol. **34**, 4651 (2000).
[45] C. M. Bethke, *The Geochemist's Workbench Release 3.0: A users guide to Rxn, Act2, Tact, React, and Gtplot* (University of Illinois, Urbana-Champaign, 1998).
[46] C. M. Bethke, *Geochemical Reaction Modeling*, 1st ed. (Oxford University Press, New York, 1996).
[47] K. J. Edwards, M. O. Schrenk, R. J. Hamers, and J. F. Banfield, Am. Mineral. **83**, 1444 (1998).
[48] K. J. Edwards, P. L. Bond, and J. F. Banfield, Environ. Microbiol. **2**, 324 (2000).
[49] M. M. McGuire, K. J. Edwards, J. F. Banfield, and R. J. Hamers, Geochim. Cosmochim. Acta **65**, 57 (2001).
[50] M. McGuire, J. F. Banfield, and R. J. Hamers, Geochem. Trans. **4** (Digital Object Identifier), 10.1039/b104111h (2001).
[51] M. P. Silverman and D. G. Lundgren, J. Bacteriol. **78**, 326 (1959).
[52] B. J. Baker, P. Hugenholtz, S. C. Dawson, and J. F. Banfield, Appl. Environ. Microbiol. **69**, 5512 (2003).
[53] P. L. Bond and J. F. Banfield, Microb. Ecol. **41**, 149 (2001).
[54] K. J. Edwards and A. D. Rutenberg, Chem. Geol. **180**, 19 (2001).
[55] R. Steudel and G. Holdt, Angew. Chem., Int. Ed. Engl. **27**, 1358 (1988).
[56] J. V. McArthur, J. E. Brofft, and L. J. Shimkets, Environ. Microbiol. **4**, 764 (2002).
[57] H. Rheims, F. A. Rainey, and E. Stackebrandt, J. Ind. Microbiol. **17**, 159 (1996).
[58] B. J. Baker, M. A. Lutz, S. C. Dawson, P. L. Bond, and J. F. Banfield, Appl. Environ. Microbiol. (in press).
[59] M. Dopson, C. Baker-Austin, P. R. Kippineedi, and P. L. Bond, Appl. Environ. Microbiol. **149**, 1959 (2004).
[60] D. E. Rawlings, H. Tributsch, and G. S. Hansford, Microbiology **145**, 85 (1999).
[61] D. A. Norris and P. R. Clark, Microbiology **142**, 785 (1996); H. Rheims, F. A. Rainey, and E. Stackebrandt, J. Ind. Microbiol. **17**, 159 (1996).
[62] D. B. Johnson and F. F. Roberto, In: Bioming: Theory, Microbes and Industrial Processes (Rawlings, D.E., Ed.), pp. 259–279.
[63] H. Hippe, Int. J. Syst. Microbiol. **2**, 501 (2002).
[64] D. B. Johnson and L. Rang, J. Gen. Microbiol. **139**, 1417 (1993).
[65] J. I. Jambor, D. K. Nordstrom, and C. N. Alpers, Sulfate Minerals—Crystallography, Geochemistry and Environmental Significance (2000), Vol. 40, p. 303.
[66] L. S. Clesceri, A. E. Greenberg, and A. D. Eaton, *Standard Methods for the Examination of Water and Wastewater/Prepared and Published Jointly by American Public Health Association, American Water Works Association, Water Environment Federation* (American Public Health Association, Washington, DC, 1996).

[67] H. H. Gerke, J. W. Molson, and E. O. Frind, J. Hydrol. **209**, 166 (1998).
[68] F. J. Zeleznik, J. Phys. Chem. Ref. Data **20**, 1157 (1991).
[69] M. A. McKibben and H. L. Barnes, Geochim. Cosmochim. Acta **50**, 1509 (1986); M. A. Williamson and J. D. Rimstidt, *ibid.* **58**, 5443 (1994); B. C. Bostick, S. Fendorf, B. T. Bowie *et al.*, Environ. Sci. Technol. **34**, 1494 (2000); C. O. Moses and J. S. Herman, Geochim. Cosmochim. Acta **55**, 471 (1991); C. L. Wiersma and J. D. Rimstidt, *ibid.* **48**, 85 (1984); M. A. A. Schoonen, A. Elsetinow, M. Borda *et al.*, Geochem. Trans. **1**, 23 (2000); A. G. Schaufauß, H. W. Nesbitt, I. Kartio *et al.*, J. Electron Spectrosc. Relat. Phenom. **96**, 69 (1998); C. M. Eggleston, J. J. Ehrhardt, and W. Stumm, Am. Mineral. **81**, 1036 (1996); J. M. Guevremont, A. R. Elsetinow, D. R. Strongin *et al.*, *ibid.* **83**, 1353 (1998); A. R. Elsetinow, M. A. A. Schoonen, and D. R. Strongin, Environ. Sci. Technol. **35**, 2252 (2001); K. M. Rosso, U. Becker, and M. F. Hochella, Am. Mineral. **84**, 1549 (1999).
[70] H. W. Nesbitt, G. M. Bancroft, A. R. Pratt, and M. J. Scaini, Am. Mineral. **83**, 1067 (1998); R. S. C. Smart, W. M. Skinner, and A. R. Gerson, Surf. Interface Anal. **28**, 101 (1999).
[71] B. Hu, Ph.D. thesis, University of Wisconsin, 2001.
[72] G. K. Druschel, Ph.D. thesis, University of Wisconsin, 2002.
[73] M. E. Hernandez and D. K. Newman, Cell. Mol. Life Sci. **58**, 1562 (2001).
[74] Y. Xu and M. A. A. Schoonen, Geochim. Cosmochim. Acta **59**, 4605 (1995).
[75] G. K. Druschel, R. J. Hamers, and J. F. Banfield, Geochim. Cosmochim. Acta (in press).
[76] G. K. Druschel, R. J. Hamers, G. W. Luther III *et al.* (unpublished).
[77] N. Okibe, M. Gericke, K. B. Hallberg, and D. B. Johnson, Appl. Environ. Microbiol. **69**, 1936 (2003).
[78] G. W. Luther, Geochim. Cosmochim. Acta **61**, 3269 (1997).
[79] G. H. Kelsall, Q. Yin, D. J. Vaughan, K. E. R. England, and N. P. Brandon, J. Electroanal. Chem. **471**, 116 (1999).
[80] M. J. Borda, A. R. Elsetinow, M. A. A. Schoonen *et al.*, Astrobiology **1**, 283 (2001).
[81] M. J. Borda, A. R. Elsetinow, D. R. Strongin *et al.*, Geochim. Cosmochim. Acta **67**, 935 (2003).
[82] G. H. Kelsall, in *Mineral Surfaces*, edited by D. J. Vaughan and R. A. D. Patrick (Chapman & Hall, New York, 1995), p. 219; M. A. A. Schoonen, Y. Xu, and D. R. Strongin, J. Geochem. Exploration **62**, 201 (1998).
[83] B. E. Taylor and M. C. Wheeler, Geochim. Cosmochim. Acta **48**, 2669 (1984); L. Toran and R. F. Harris, *ibid.* **53**, 2341 (1989).
[84] R. R. Seal III, in *Environmental Aspects of Mine Wastes*, edited by J. I. Jambor, D. W. Blowes, and A. I. M. Ritchie (Mineralogical Association of Canada, Ottawa, 2003), Vol. 31, p. 430.
[85] P. R. Holmes and F. K. Crundwell, Hydrometallurgy **39**, 353 (1995).
[86] N. Kishimoto, Y. Kosako, and T. Tano, Curr. Microbiol. **22**, 1 (1991).
[87] G. Darland, T. D. Brock, W. Samsonof *et al.*, Science **170**, 1416 (1970); A. Segerer, T. A. Langworthy, and K. O. Stetter, Syst. Appl. Microbiol. **10**, 161 (1988).
[88] G. W. Tyson, J. Chapman, P. Hugenholtz, E. E. Allen, R. J. Ram, P. M. Richardson, V. V. Solovyev, E. M. Rubin, D. S. Rokhsar, and J. F. Banfield, Nature (London) **428**, 37 (2004).
[89] K. J. Edwards, P. L. Bond, G. K. Druschel *et al.*, Chem. Geol. **169**, 383 (2000).